Risø-R-1283(EN)

# Association Euratom – Risø National Laboratory Annual Progress Report 2000

Edited by J.P. Lynov and B.N. Singh



Risø National Laboratory, Roskilde, Denmark
August 2001

**Abstract** The programme of the Research Unit of the Fusion Association Euratom - Risø National Laboratory covers work in fusion plasma physics and in fusion technology. The fusion plasma physics group has activities within development of laser diagnostics for fusion plasmas and studies of nonlinear dynamical processes related to turbulence and turbulent transport in the edge region of magnetised fusion plasmas. The activities in technology cover investigations of radiation damage of fusion reactor materials. These activities contribute to the Next Step, the Long-term and the Underlying Fusion Technology programme. A summary is presented of the results obtained in the Research Unit during 2000.

ISBN 87-550-2917-5
ISBN 87-550-2918-3 (Internet)
ISSN 0106-2840

Print: Pitney Bowes Management Services Danmark A/S, 2001

# Contents

# 1. Research Unit

The activities in the Research Unit cover two main areas:

**Fusion Plasma Physics** which includes:

- *Experimental turbulence studies.* Development of laser diagnostics for spatially localised turbulence measurements. In collaboration with IPP Garching measurements are being performed on the W7-AS stellarator with a collective scattering diagnostic built at Risø. In 2000, turbulence studies have also been carried out in collaboration with Culham on MAST using a microwave reflectometer.
- *Theoretical and numerical turbulence studies.* For the interpretation of the results from the laser diagnostic, extensive computer simulations are carried out of plasma density fluctuations under various types of electrostatic turbulence. Numerical simulations are also used for studies of nonlinear plasma processes of relevance to turbulent transport and internal transport barriers.

**Fusion Technology** which includes:

- Experimental and theoretical investigations of the effects of irradiation on the microstructural evolution and on the physical and mechanical properties of metals and alloys relevant to the Next Step, the Long Term and Underlying Fusion Technology Programme.

The **global indicators** for the Research Unit in 2000 are:

| | | |
|---|---|---|
| • Professional staff | 9.8 | man-years |
| • Support staff | 5.3 | man-years |
| • Total expenditure - incl. mobility | 2.16 | MioEuro |
| • Total Euratom support | 0.53 | MioEuro |

# 2. Fusion Plasma Physics

## 2.1 Introduction

The activities in this area have been carried out under the Plasma Physics and Fluid Dynamics Programme in the Optics and Fluid Dynamics Department. The main objective of the research is to contribute to the understanding of turbulent transport in fusion plasmas. In the work towards this objective, the programme interacts with other activities in the department in the fields of optics and fluid dynamics to the mutual scientific benefit of the projects involved.

The main results obtained during 2000 can be summarised as follows:

The Risø laser diagnostic, named LOTUS, on the Wendelstein 7-AS stellarator at IPP-Garching has been modified as a consequence of the installation of the new divertor in W7-AS. At the same time the diagnostic has been upgraded. Results obtained with the new set-up are presented. Experimental investigations of plasma turbulence have also been carried out in collaboration with Culham on the MAST experiment, in this case by means of the MAST microwave reflectometer. Risø's most advanced numerical code, named TYR, for first-principle modelling of plasma turbulence in the edge region of large-scale fusion devices has been benchmarked against a similar code from IPP-Garching in linear and weakly non-linear regimes with excellent agreement. Our numerical codes for plasma turbulence have also been successfully validated against plasma experiments conducted in Kiel. These experiments have provided important new results concerning the possibility of controlling plasma turbulence. Purely theoretical and numerical investigations of plasma turbulence have also been carried out at Risø with emphasis on the dynamical interplay between internal transport barriers, zonal flows and turbulent transport.

In this report, a brief description is included of three special projects, which are derived from the main scientific programme. These projects are: 1) pellet injectors, 2) industrial spin-off of laser anemometers for wind turbines and 3) lectures in plasma physics.

## 2.2 Experimental turbulence studies

### 2.2.1 Upgrade of and measurements using the LOTUS diagnostic

*N. P. Basse, S. Zoletnik* (*CAT-Science, Budapest, Hungary), M. Saffman***
*(**Department of Physics, University of Wisconsin, USA), M. Endler****
*(*** Max-Planck-Institut für Plasmaphysik, Teilinstitut Greifswald, Germany),*
*P.K. Michelsen, B.O. Sass, J.C. Thorsen and H.E. Larsen*

The 1999 Wendelstein 7-AS (W7-AS) campaign came to an end in August 1999. The purpose of the subsequent shutdown was to install the so-called 'island divertor' system in the machine, which is designed to be optimised for $\iota_a$ = 5/9 plasma operation (see Ref. 1 and references therein). The shutdown allowed us to make a series of improvements to the LOTUS (LOcalised TUrbulence Scattering) density fluctuation diagnostic, including:

- New acquisition rack with improved laser shutter system and other safety systems
- Upgrade of laser exciter (new high-voltage resistors, new current control card)

- New laser stabilisation system using a photovoltaic detector and modulation of the laser output mirror
- Optical rail to ease alignment on the vertical transmitting table in the W7-AS basement
- Lens holders for modified diagnostic position
- Computer upgrade

The work on these improvements predominantly took place at Risø during the autumn of 1999 and the spring of 2000.

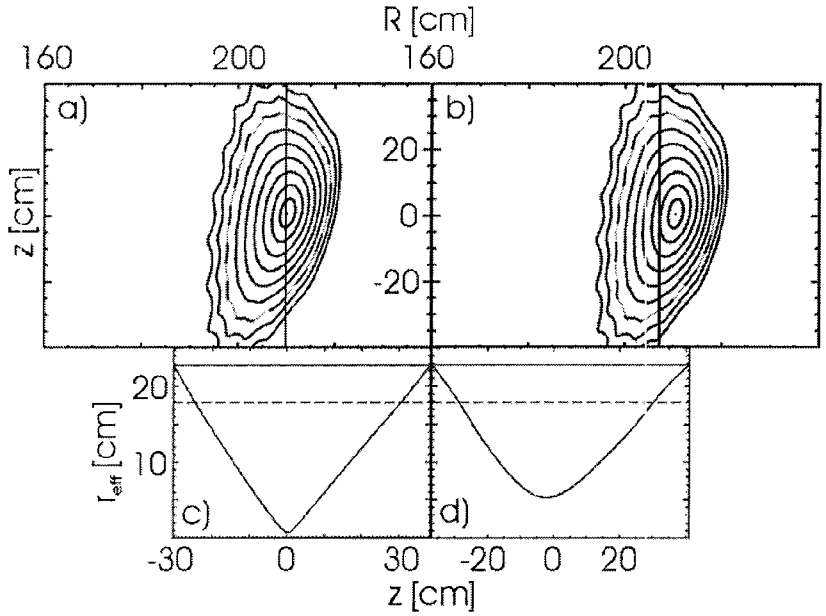


Figure 1. Comparison of measurement position relative to $\iota_a = 0.344$ flux surfaces in 1999 (inset a, R = 209.8 cm) and 2000 (inset b, R = 207.2 cm). The vertical lines indicate the approximate measurement volume position. Insets c and d show the effective radial coordinate $r_{eff}$ along the vertical measurement volumes. The dashed lines show the last closed flux surface, and the dotted lines show the plasma boundary.

The divertor installation meant that one of the modules was placed directly above our lower access port. In collaboration with IPP-Garching,[2] a hole was made in one of the recessed tiles to allow our four laser beams to pass through. The hole is rectangular (40 mm in the toroidal direction $\varphi$ and 42 mm in the major radius direction $R$) with an addition to allow extra flexibility. The limitation posed by the divertor (previously full access through a 200 mm diameter window) means that it is no more possible to measure with one wide measurement volume; measurements are now resticted to two narrow volumes. The centre of the hole has been displaced with respect to the centre of the window; inward along $R$ by 19.5 mm, toroidally by 33.1 mm. The toroidal change is very slight compared with a machine circumference of about $2\pi R \sim 12500$ mm, but the major radius change is more significant as can be seen in Figure 1.

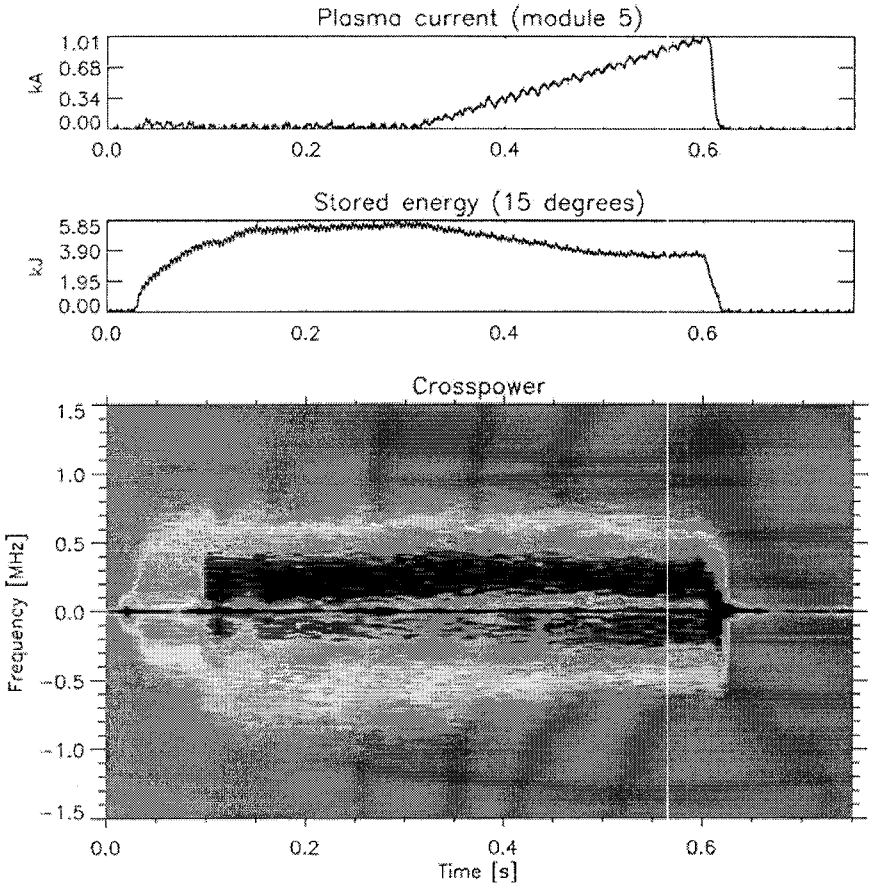


Figure 2. From top to bottom: Net plasma current, stored energy and crosspower amplitude (linear scale) versus frequency and time. The wave number of the density fluctuations measured was 20 $cm^{-1}$. The relative angle between the volumes $\theta_R = 4$ degrees (centre of plasma, shot 50031).

We now briefly discuss the dedicated experimental programme in the 2000 campaign. In 1999 we made a series of experiments to investigate the changes of density fluctuations during slow current induced confinement transitions.[3] The initial plan was to redo previous experiments with the modified set-up, but due to in-vessel diagnostics and a bad torus conditioning (boronisation was impossible because of the planned December 2000 opening) a number of plasma parameters were changed. However, it was still possible to construct discharges where a slow current ramp induces a gradual confinement degradation. The main plasma parameters were: $\iota_a = 0.350$, $B_\varphi = 2.5$ T, $B_z = 12$ mT, 450 kW central ECR heating, deuterium gas, $n(r_{eff}=0) \sim 7\times10^{19}$ $m^{-3}$ and $T_e(0) \sim T_i(0) \sim 1.3$ keV. A series of seven similar shots (#50031-50037) was made, where we changed the relative position of the measurement volumes between each one. An example of the measurements is shown in Figure 2. We measured density fluctuations at 20 $cm^{-1}$; the measurement volume separation was 19 mm, and the volume diameter (two times waist) was 7 mm. The top plot shows the plasma current in kA. This was compensated to zero for the first 300 ms of the discharge and thereafter slowly ramped up to 1 kA (at 600 ms). The centre plot shows the corresponding stored energy in kJ. The maximum confinement is reached just before the current ramp is initiated at 300 ms. From that point on, the stored energy drops slowly in response to the current induced change of $\iota_a$. The colour contour plot shows the crosspower amplitude between the two LOTUS measurement volumes on a linear scale versus frequency and time. Positive/negative frequencies are fluctuations travelling radially outward/inward along *R*. It is clear that there is

a spin-down and amplitude increase of the two features having opposite frequencies as has been reported previously.[4] However, the interpretation is difficult because too many factors have been changed compared with our baseline experimental configuration. Moreover, the plasma confinement is extremely sensitive to changes around the $\iota_a = 0.35$ 'edge' of W7-AS. An additional complication is that the separation of the measurement volumes has now become so small that the dual beam localisation technique is compromised. To facilitate a direct comparison between these and previous results, Figure 3 shows the crosspower amplitude for a slow current ramp discharge in 1999 (adapted from Ref. 4). Figure 2 and Figure 3 both show density fluctuations originating at the bottom of the plasma, but due to a reorientation of the two beams creating the measurement volumes the features have swapped frequency sign. During the next experimental W7-AS campaign, which is to commence in March 2001, we will redo the experiments with parameters identical to those of the 1999 experiments. This will hopefully clarify the impact of the changed diagnostic position.

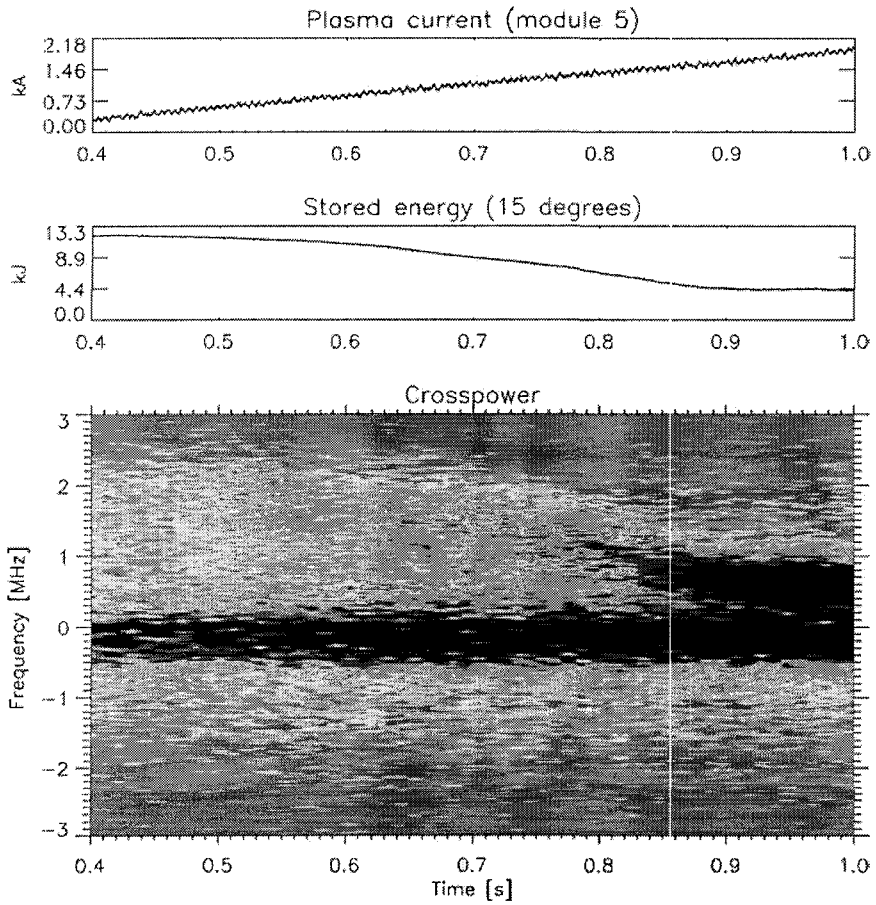


Figure 3. From top to bottom: Net plasma current, stored energy and crosspower amplitude (linear scale) versus frequency and time. The wave number of the density fluctuations measured was 15 $cm^{-1}$. The relative angle between the volumes $\theta_R = 10.5$ degrees (bottom of plasma, shot 47940).

1. K.McCormick et al., Plasma Phys. Control. Fusion **41** (1999) B285.
2. Bertram Brucker (2000) Private communication.
3. R.Brakel et al., Plasma Phys. Control. Fusion **39** (1997) B273. R.Brakel et al., 25th EPS, ECA **22C** (1998) 423.
4. N.P. Basse et al., 27th EPS ECA **24B** (2000) 940.

### 2.2.2 Density fluctuation measurements in the Mega Amp Spherical Tokamak

*S. B. Korsholm and G. Cunningham (Culham Science Centre, Abingdon, Oxfordshire, UK)*

The control of plasma transport is essential in the development of fusion energy as a power source. Transport of energy and particles out of a plasma has experimentally been shown to be governed by turbulent transport. An understanding of the plasma turbulence is thus important.

Previously, the study of turbulence had mainly been performed analytically and numerically, but over the last decade an increasing effort has been made to investigate plasma turbulence experimentally. Ideally, these investigations would require simultaneous measurements of small-scale fluctuations in the plasma temperature, density, electric potential, ion velocities and magnetic flux as well as the individual phase relationships. Such measurements are beyond the scope of present-day technology, despite the use of many different diagnostics. The measurements of some of the plasma properties, however, are possible and this year Risø staff has been involved in running the fluctuation reflectometer at the newly built Mega Amp Spherical Tokamak (MAST) located at Culham Science Centre, UK.

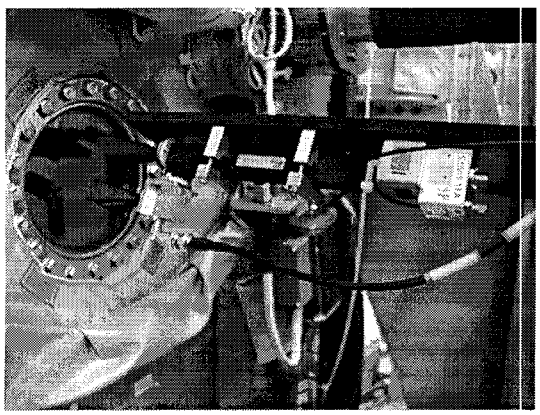

Figure 4. The MAST fluctuation reflectometer.

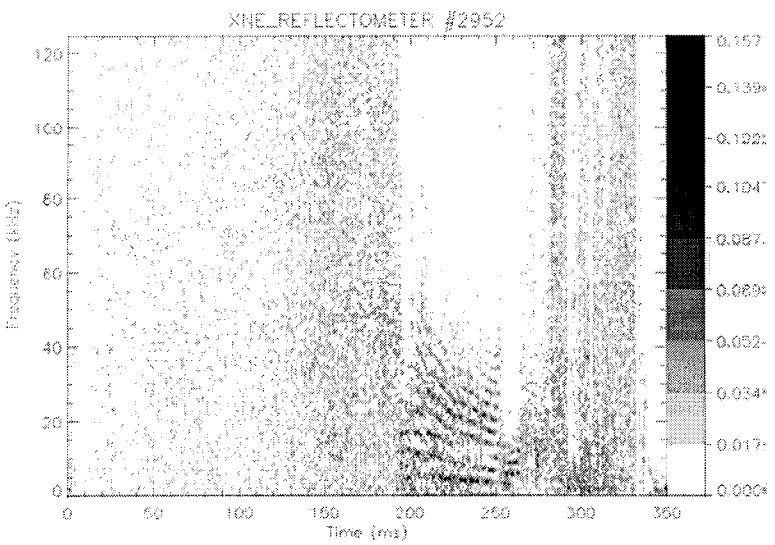


Figure 5. Spectrogram of MAST shot no. 2952 where the H-mode starts at t = 195 ms and a low frequency mode structure builds up. Data from the MAST fluctuation reflectometer.

The experimental set-up is illustrated in Figure 4, where the MAST vessel is seen to the left. The system proved good at detecting H-modes (high confinement modes), which is illustrated in Figure 5. Future developments will include expansion to four frequency channels, and extension of the measured frequencies up to 6 MHz.

## 2.3 Theoretical and numerical turbulence studies

### 2.3.1 Benchmarking 3D codes of drift-Alfven turbulence

*V. Naulin and B.D. Scott (Institut für Plasmaphysik, Garching, Germany)*

The Risø TYR code has been developed to model plasma turbulence in the edge region of large-scale fusion devices. It includes the dynamics of drift-wave turbulence and the effects of the complex equilibrium magnetic field structure of toroidal devices. The code has recently been extended from an electrostatic 3-field model to a 5-field electromagnetic model with parallel Alfven dynamics considered. Density, electrostatic potential as well as current and parallel ion-velocity fluctuations are included. To test and verify the code and to gain insight into strengths and weaknesses of the underlying numerical schemes, the code is benchmarked against the DALF family of codes developed by Bruce Scott at the IPP Garching. Benchmarking of these kinds of codes gets more and more necessary as the code complexity increases. For plasma turbulence simulations, systematic benchmarkings have not yet been established. Thus, a large number of test runs were conducted in various regions of the parameter space. For the linear and weakly non-linear regimes excellent agreement between the codes was found. Figure 6 shows the initial linear wave structure in a sheared magnetic field, close to a resonant flux surface. In a second campaign the non-linear properties of both codes will be addressed. A focus of the benchmarking is on the electromagnetic effects, which are difficult to include into a code in a stable manner, but which have proved to be of importance to the scaling of, e.g., the transport.

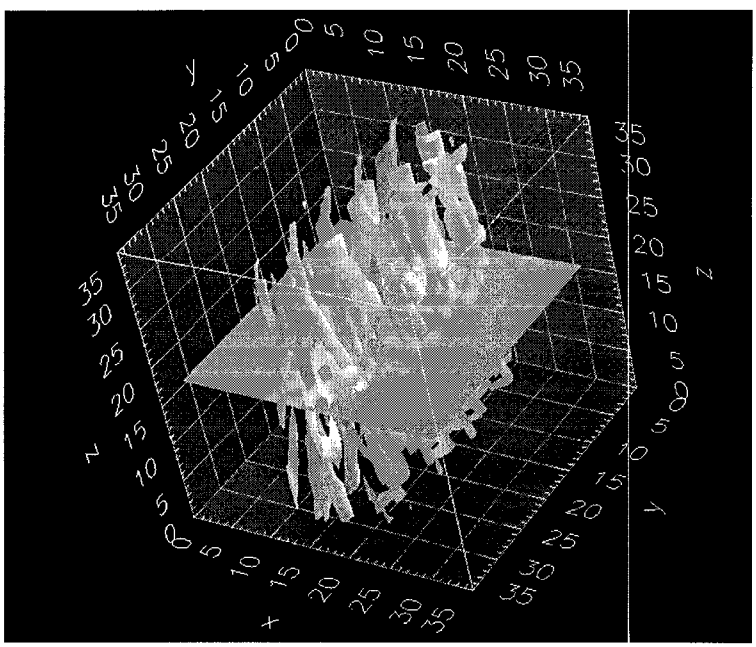


Figure 6. Density fluctuations in a sheared magnetic field. The alignment of the fluctuations with the magnetic field structure and initial localisation at the resonant flux surface can be clearly seen.

### 2.3.2 Taming drift-wave turbulence

*C. Schröder*, T. Klinger* (*Institut für Physik, Ernst-Moritz-Arndt Universität Greifswald, Germany), D. Block**, A. Piel** (**Institut für Experimentelle und Angewandte Physik, Christian-Albrechts Universität Kiel, Germany), G. Bonhomme (Laboratoire de Physique des Millieux Ionisés, Université Henri Poincaré Nancy, France) and V. Naulin*

Drift wave turbulence is basically a spatiotemporal phenomenon and, thus, it is barely expected that a purely temporal or spatial control technique proves to be efficient and robust. A number of experiments on temporal feedback stabilisation of plasma instabilities have been reported, with often ambiguous conclusions. Recently, the suppression of several drift-type instabilities has been demonstrated in a linear device.[1] However, control was achieved by rather violent changes of global plasma parameters, which may be costly or even impossible in other cases.

An alternative approach is "control of chaos",[2] where unstable periodic states, embedded in chaos, are stabilised by only tiny adjustments of one or more accessible parameters. The success of this conception has been demonstrated for various different plasma waves and instabilities.[3] Using a continuous, temporal feedback technique, a chaotic drift wave state has successfully been controlled by weak parameter perturbations.[4] Unfortunately, low-dimensional chaotic behaviour is rather exceptional for drift waves, since their complex dynamics tends to be of turbulent nature. A much more promising strategy to tame drift wave turbulence over a wide parameter range is open-loop synchronisation acting in both space and time.[2,5] We have conducted experiments and numerical simulations on open-loop synchronisation of drift wave turbulence in a magnetized plasma with cylindrical geometry. For the synchronization experiments an arrangement of eight stainless-steel electrodes (octupole exciters) is placed in flush-mounted geometry in the edge region of the plasma column. Using a phase shifted time-dependent bias, this enables us to imprint specific waves at specific frequencies. For the numerical simulations an extension of the Hasegawa-Wakatani model is used in 2D disk geometry, with the outer drive modelled as a parallel current. Both experiment and numerical simulation show that relatively weak exciter signals synchronise turbulent drift wave states and, thereby, establish the preselected single-drift mode if the later is in resonance with a naturally excited wave (see Figure 7 and Figure 8).

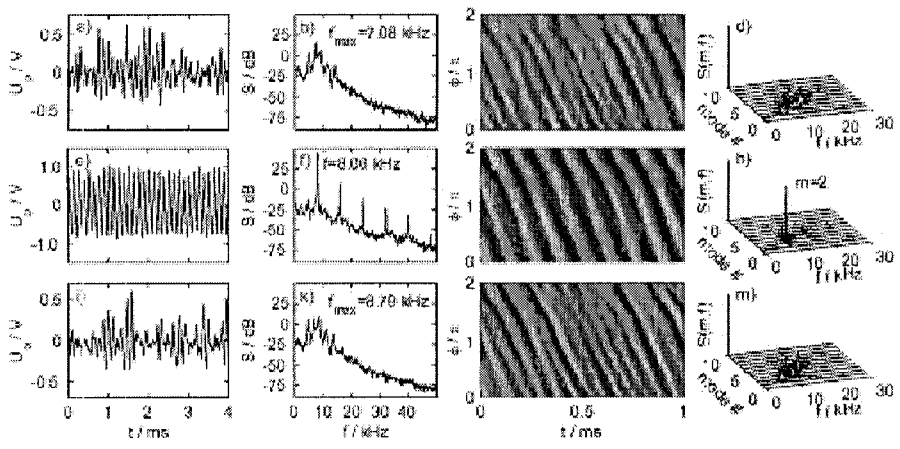


Figure 7. Temporal and spatiotemporal drift wave dynamics: experiment. The three rows correspond to the unperturbed case, active exciter with a co-rotating field and active exciter with counter-rotating field, respectively. The four columns show the density fluctuations, the frequency power spectrum, the spatiotemporal density fluctuations and the frequency mode number power spectrum. Power spectra are obtained by Fourier transformation of the temporal and spatiotemporal data.

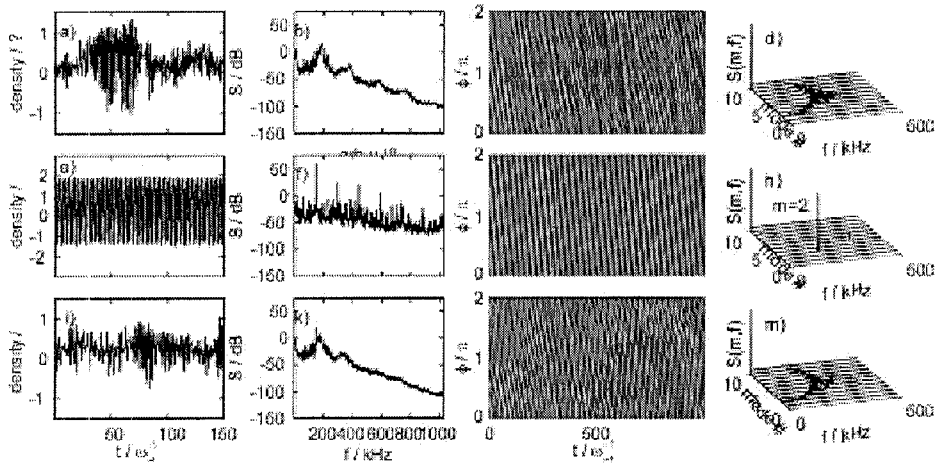

Figure 8. Temporal and spatiotemporal drift wave dynamics: simulation.The figure is arranged as in Figure 7. Excellent agreement is found between experiment and simulation.

The numerical solution allows access to the complete fields and the transport (Figure 9).

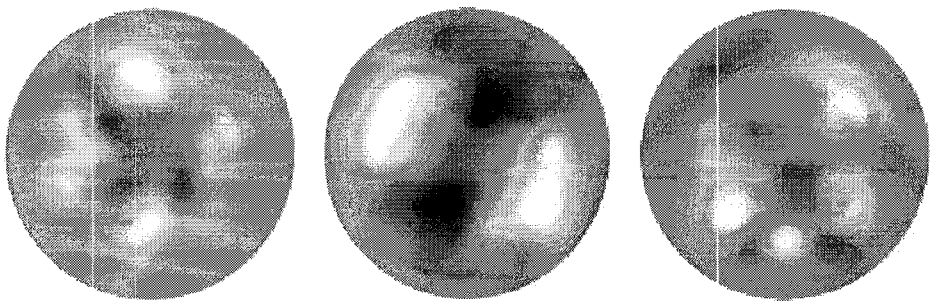

Figure 9. Snapshots of the 2D mode structure as taken from the simulations. Grey scale plots of the density fluctuations; from left to right: Unperturbed case, co- and counter-rotating current profiles.

This is an important step towards control of this kind of turbulence. 3D simulations are underway to establish the effect on transport and to better relate to experimental parameters.


1. A. K. Sen, J. S. Chiu, J. Chen, and P. Tham, Plasma Phys. Control. Fusion **39**, A333 (1997).
2. H. G. Schuster, editor, *Handbook of Chaos Control*, VCH-Wiley, Weinheim, 1999.
3. T. Klinger et al., Phys. Rev. Lett. **79**, 3913 (1997).
4. E. Gravier, X. Caron, and G. Bonhomme, Physics of Plasmas **6**, 1670 (1999).
5. T. Shinbrot, Advan. Phys. **44**, 73 (1995).


### 2.3.3 Comparison of simulations with simple plasma experiments


*V. Naulin, D. Block*, O. Grulke*, F. Greiner*, S. Niedner*, A. Piel* and U. Stroth**
*(*Christian-Albrechts Universität Kiel, Germany)*


Small-sized plasma experiments with a simple geometry are an ideal playground to test various hypotheses concerning, e.g., plasma transport and the appearance of coherent structures in these nearly 2D systems. Well-developed diagnostics and good control of the experiments make it possible to verify numerical codes with these experiments. Their relatively low plasma temperatures put the relevant spatial sizes in a range where today's

numerical resolution is sufficient to simulate the whole plasma cross-section. At Kiel University probe measurements of the linear experiment KIWI and the simple magnetised torus TEDDI will be compared with results from Risø's 2D and 3D codes. Information about coherent structures, turbulent transport and statistical properties of the plasma turbulence shall be obtained. Plasma properties that are difficult to access, such as three-dimensional mode structures and transient transport events, will be made available from the numerical simulations.

### 2.3.4 Anomalous diffusion of particles and the relation to transport in vortex-dominated turbulence

*V. Naulin, Th. Jessen, P. Michelsen, A. H. Nielsen and J. Juul Rasmussen*

The turbulent diffusion in vortex-dominated 2D turbulence is found to be well described by a random-walk process with at least two different step lengths and durations in each of the two directions, parallel and perpendicular to a background density gradient. One set is given by the characteristic linear times and length scales of the wave motion, the other is determined by the trapping times and the vortex velocities. The appearance of two different sets of scales for the Brownian motion corresponds to anomalous diffusive behaviour. For realistic drift-wave turbulence it is found to result in superdiffusion in the direction of the wave propagation and sub-diffusion along the gradient.[1]

Having determined the particle diffusion coefficient, the question arises how this compares with the anomalous ExB-flux $\Gamma = < \tilde{u} \tilde{v}_r >$ for the case of drift-wave turbulence. Using the conservation of potential vorticity a condition can be derived showing the equivalence for particle diffusion and density transport. However, we find that if the turbulence is caused by an external drive, this relation no longer holds. Then one can have finite mixing and particle diffusion due to the turbulence D > 0 and exactly zero flux. This severely limits the applications of Hasegawa-Mima type equations to describe particle diffusion and transport.

1. V. Naulin, A.H. Nielsen and J. Juul Rasmussen, Phys. Plasmas 6, 4575 (1999).

### 2.3.5 Turbulent equipartition and dynamics of transport barriers in electrostatic turbulence

*V. Naulin, J. Nycander (FOA, Stockholm, Sweden) and J. Juul Rasmussen*

The generation of large-scale flows by the rectification of small-scale turbulent fluctuations is of great importance both in fluids, e.g. geophysical flows, and in magnetically confined plasmas.[1] The usually sheared flows act back on the turbulence by shearing apart and, thereby, suppressing fluctuations on all scales, thus setting up transport barriers.

In hot magnetised plasmas the main cross-field transport is anomalous and ascribed to low-frequency electrostatic fluctuations. It is generally recognised that self-consistently developing large-scale poloidal - or zonal - flows strongly reduce the radial turbulent transport by "quenching" the turbulence. This mechanism may be responsible for some forms of confinement enhancements in magnetically confined plasmas, e.g. the celebrated H-mode regime.

Since the turbulence and the associated transport cannot be avoided, it is essential to understand how the zonal flows - the transport barriers – develop and control the turbulence as well as the transport.

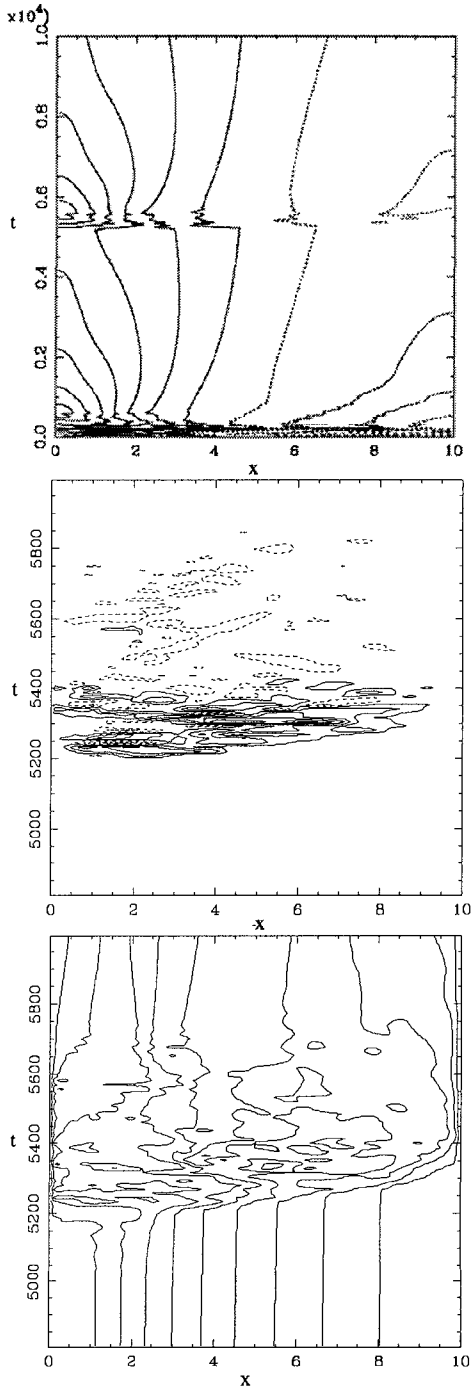


Figure 10. Upper panel: Contours of the zonal velocity, V, over time. Middle and lower panels: Enlarged with respect to time for the flux burst $\Gamma_T(t)$ plotted versus (x,t) and the temperature profile over time.

We investigate the evolution of turbulence and the associated formation of transport barriers – zonal flows - in a model system for 2D electrostatic pressure-driven flute modes in an inhomogeneous magnetic field. The fluctuations are flux driven and supplied via a Rayleigh-Taylor instability setting in when the pressure gradient exceeds the magnetic field strength gradient. This pressure gradient is forced by a constant temperature difference

between the two sidewalls of the computational domain. The temperature difference is sustaining a thermal flux.[2]

Turbulent equipartition predicts the background profiles and gradients resulting from the homogenisation of the Lagrangian invariants due to the strong mixing by the turbulence. This is clearly revealed for large aspect ratios, $L_y/L_x > 3.8$ , where x is in the direction of the gradients ("radial direction") and y is perpendicular to the gradients ("poloidal direction") (the confining magnetic field is in the z-direction). These profiles are flatter than the profiles that will result from classical viscous diffusion in the absence of the turbulence. For small aspect ratio, however, the numerical simulations show a strong tendency for the evolution of a poloidal shear flow that quenches the effective turbulent mixing and the transport changes from being anomalous, i.e. fluctuation driven, to being diffusive. Thus, a much steeper gradient evolves on a diffusive timescale. Subsequently, the resulting steep gradient is prone to the Rayleigh-Taylor instability again and short burst-like destabilisation occurs locally whereby the profiles are flattened out. The transport associated with these burst-like events propagates down the background gradient and has properties of avalanche-like events. This behaviour is illustrated in Figure 10.

In the upper panel we show the evolution of poloidal flow by plotting the contours of the velocity V in the x-t plane. A regular zonal flow is seen to establish at around t = 100 and to dominate the evolution for a long period, where the turbulence is suppressed. The flow is slowly decaying and at t = 5200 it has become weak enough to allow the build-up of the turbulence again. This is accompanied by a strong burst in the thermal flux, as seen in the second panel, and the temperature profile is flattened out again (see the last panel).

1. P.W. Terry, Rev. Mod. Phys. **72**, 109 (2000).
2. V. Naulin, J. Nycander and J. Juul Rasmussen, Phys. Rev. Lett. **81**, 4148 (1998)

### 2.3.6 Shear flow stabilisation of pressure driven flute modes

*E.S. Benilov (Dept. Mathematics, University of Limerick, Ireland), V. Naulin and J. Juul Rasmussen*

Global flows with sheared velocity profiles are generally found to have profound influence on the evolution of a class of Rayleigh-Taylor like instabilities (RTI). This has been discussed both in the context of neutral fluids, where the RTI appears in cases with an inverted stratification so that heavier fluid is "resting" on top of lighter fluid, and in the context of magnetised plasmas, where the pressure gradient perpendicular to the magnetic field is stronger than the magnetic field gradient.

We have considered the eigen-value problem governing the stability properties of these situations. In the long wave limit the plasma and fluid cases reduce to a similar equation. To be specific, we consider a parallel flow in a density-stratified ocean in such a way that both streamlines and surfaces of equal density are horizontal. In the plasma case this corresponds to a flow (in the y-direction) perpendicular to the pressure gradient (in the x-direction) and to the magnetic field (in the z-direction) with a gradient in the x-direction. By linearising the governing equations we obtain an equation corresponding to the Taylor-Goldstein equation[1] for the x-variation of the stream function. Generally, it is found that the sheared flow acts destabilizingly; i.e., on an infinite domain it will extend the region of instability. We have, however, found that for realistic density/pressure profiles ($tanh(x)$) and with fixed boundaries in the x-direction sheared flows may act stabilisingly for part of the wave number spectrum. This is illustrated in Figure 11 where a shear flow with the profile $U = U_0\ tanh(x)$ is applied. The RTI is not completely suppressed, but short wavelengths (in the y-direction) are stabilised, and the shear flow has introduced a finite $k_c$ so that perturbations with $k > k_c$ are

stabilised. Similar behaviour is found for a linear shear flow $U = U_0 x$. This will imply that for a system with a finite period in the y-direction the RTI may be stabilised when the period $L < 2\pi/k_c$.

1. J.W. Miles, J. Fluid Mech. **10,** 496 (1961) and L.N. Howard, J. Fluid Mech. **10,** 509 (1961).

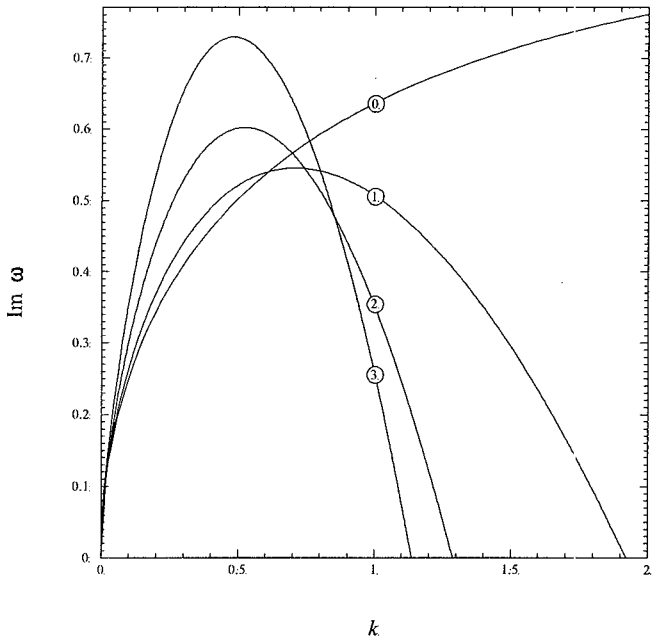


Figure 11. Growth rate of the zeroth (most unstable) mode versus wave number for an inverted stratification. The curve numbers correspond to the value of $U_0$.

### 2.3.7 Reynolds stress and shear flow generation

*S. B. Korsholm, V. Naulin, J. Juul Rasmussen, P. K. Michelsen and L. Garcia*
*(Universidad Carlos III and CIEMAT, Madrid, Spain)*

One of the major challenges in the research towards a fusion power plant is the understanding and control of the plasma turbulence leading to anomalous transport of particles and energy.

Experimentally obtained confinement schemes such as H-mode confinement regimes show a drastically reduced radial transport. The generation of H-mode confinement regimes seems to be closely related to poloidal shear flows in the edge region of the plasma. Generally, it is observed experimentally and in numerical models that shear flows in plasmas suppress turbulence and transport. The generation mechanism of these flows is thus of great interest. In this numerical work we investigate the relation between the so-called Reynolds stress[1] and the poloidal flow generation.

The model used in the numerical investigations is the three-dimensional drift wave Hasegawa-Wakatani model.[2] The simulations are performed in a slab geometry periodic in $y$ and $z$ (corresponding to the poloidal and toroidal directions, respectively), while we use non-permeable walls in the radial direction, $\phi(x=0)= \phi(x=L_x)=0$ and $n(x=0)=n(x=L_x)=0$, i.e. Dirichlet boundaries in $x$. $\phi$ is the electrostatic potential fluctuations, n is the density fluctuations and $L_x$ is the domain length. The simulations are performed using pseudo-spectral methods.

The Reynolds stress is a measure of the anisotropy of the turbulent velocity fluctuations that produce a stress on the mean flow. This may cause acceleration of the flow in the plasma, which, e.g., could be a poloidal flow ($y$-direction). The Reynolds stress is defined as:

$$\mathrm{Re}_\phi = - < v_x v_y >_{y,z} = \left\langle \frac{\partial \phi}{\partial y} \frac{\partial \phi}{\partial x} \right\rangle_{y,z} .$$

To determine the Reynolds stress one needs accurate measurements of the potential perturbations. However, accurate measurements of the potential perturbations are quite difficult, and nearly impossible in hot plasmas in large devices. Thus, a pseudo-Reynolds stress based on much easier obtainable density measurements is investigated. The pseudo-Reynolds stress is defined as:

$$\mathrm{Re}_n = \left\langle \frac{\partial n}{\partial y} \frac{\partial n}{\partial x} \right\rangle_{y,z} .$$

We find that the Reynolds stress $\mathrm{Re}_\phi$ and the pseudo-Reynolds stress $\mathrm{Re}_n$ are strongly correlated with a correlation of 0.8. The reason for the strong correlation between $\mathrm{Re}_n$ and $\mathrm{Re}_\phi$ is that the density and the potential fluctuations are strongly correlated for drift waves.

The conclusion of this work is that the pseudo-Reynolds stress may give a good estimate of the real Reynolds stress and it may therefore be possible to predict flow generation by measuring density fluctuations. In Figure 12 below we compare the poloidal flow with the flow predicted by the pseudo-Reynolds stress. The observed behaviour may, however, be specific to this particular turbulence model and more models have to be investigated.

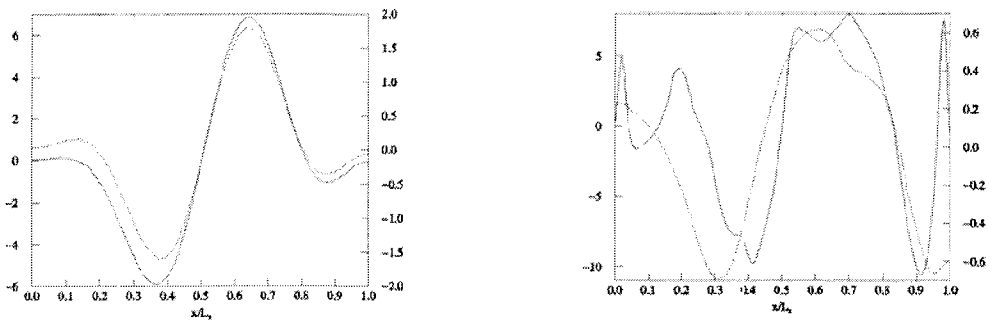

a) b)

Figure 12. The poloidal flow (dashed line) compared with the flow predicted by the drift wave pseudo-Reynolds stress (full line) at two instants in time a) t = 75 and b) t = 125.

Finally, we have looked into the effect of a misaligned probe array for determination of the Reynolds stress. It was found that the probe array in an experiment should be aligned with the magnetic field within 5-7° in order to get a good estimate of the Reynolds stress. This criterion should be possible to fulfil. In Figure 13 a schematic presentation of the probe array used in the numerical investigations is given, as well as the results of the misalignment calculations.

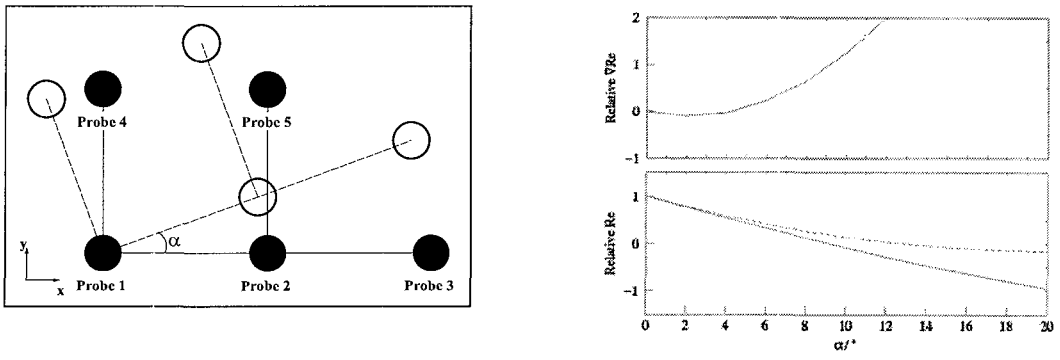


a) b)

Figure 13. a) The probe array used in the numerical investigations of the effects of misalignment. b) The upper graph shows the difference of the "measured" divergence of the Reynolds stress and the value for perfect alignment relative to the latter as a function of the misalignment angle α. The lower graph shows the change of the Reynolds stresses measured by probes 1, 2, 4 (full line) and probes 2, 3, 5 (dashed line) relative to the Reynolds stresses for perfect alignment.

1. D. J. Triton, *Physical Fluid Dynamics*, Clarendon Press, Oxford, 2nd ed., 1988, Chapter 19.
2. A. Hasegawa and M. Wakatani, Phys. Rev. Lett. **50** (1983) 682-686.

# 2.4 Special projects
## (not financially supported by the Euratom – Risø Association)

### 2.4.1 Pellet injectors

*P.K. Michelsen and B. Sass*

Technical support to the groups that still have Risø-made pellet injectors has continued. The 8-shot pellet injector that was designed and produced at Risø more than ten years ago to the Dutch tokamak RTP at the FOM-Institute was recently transferred to MAST (Mega Amp Spherical Tokamak) at Culham Science Center, UK. After an initial test of the injector, the main injector unit was brought to Risø where all the gun barrels were changed to new ones with larger but different diameters in order to get larger pellets. A new cryostat was also installed and the whole unit was reconditioned. After returning to Culham the injector was successfully tested. The plan is to connect the injector to MAST with a very long and curved guide tube since the injector is located in a small room next to the torus hall.

### 2.4.2 Laser anemometry for wind turbines

*R. Skov Hansen and S. Frandsen (Wind Energy and Atmospheric Physics Department)*

As a spin-off from the work on laser plasma diagnostics based on collective scattering, a project on long-range wind velocity measurements for power curve determination and wind turbine control was initiated. This project is supported by the EU Joule programme, and the partners include the world's largest manufacturer of wind turbines, *NEG-Micon* (Denmark), a major manufacturer of $CO_2$ lasers, *Ferranti Photonics Ltd.* (United Kingdom) and a small-and medium-size enterprise *WEA Engineering* (Denmark).

In 2000, an autodyne detection system has been investigated, and it was demonstrated that this method was not suited for the present laser anemometer due to the physics of the $CO_2$ laser. The laser anemometer will instead be based on a simplified heterodyne detection set-up, where the reference wave is established by reflecting a small fraction of the output laser beam back into the instrument. This scheme has been successfully tested with a 6W laser both under laboratory conditions and in the field. The system has not yet been mounted on the top of a wind turbine. In the process of developing the instrument, it has been realized that the proposed selling price of the instrument will be considerably higher than believed when planning the project. Several alternative solutions to this problem are now under consideration.

### 2.4.3 Lectures in plasma physics

*P.K. Michelsen*

A course in fundamental Fusion Plasma Physics is given regularly every autumn semester. The course in taught in 27 double lectures either in Danish or English if these are English-speaking students. The book *Introduction to Plasma Physics* by R.J. Goldston and P.H. Rutherford is used for most of the course. The students finish the study by an oral examination. A special course in Fusion Reactor Physics was given during the spring semester 2000 with a three-day study tour to Culham and JET included. Another special course in stellarator physics was given in the autumn semester 2000 with a three-day study tour to IPP-Garching.

## 2.5 Participants in Fusion Plasma Physics

### 2.5.1 Scientific staff

Dinesen, Palle (from 1 October)
Glückstad, Jesper (part time)
Larsen, Henning (part time)
Lynov, Jens-Peter (part time)
Michelsen, Poul
Naulin, Volker
Nielsen, Anders
Rasmussen, Jens Juul

### 2.5.2 Post doc

Dinesen, Palle (until 30 September)

### 2.5.3 PhD students

Basse, Nils
Korsholm, Søren

### 2.5.4 Technical staff

Astradsson, Lone
Jessen, Martin
Sass, Bjarne
Thorsen, Jess

### 2.5.5 Guest scientists

Benilov, Eygene S., University of Limerick, Ireland
Hesthaven, Jan, Brown University, Rhode Island, USA
Scott, Bruce, IPP-Garching, Germany
Wyller, John, Agricultural University of Norway, Norway

### 2.5.6 Short-term visitors

Anderson, Johan, Chalmers University of Technology, Sweden
Annibaldi, Silvia Valeria, School of Cosmic Physics, Dublin Institute for Advanced Studies, Ireland
Bergé, Luc, Commissariat à l'Energie Atomique, Centre d'Etudes de Limeil-Valenton, France
Block, Dietmar, Christian Albrechts Universität zu Kiel, Germany
Germaschewski, Kai, University of Düsseldorf, Germany
Gloria, Falchetto, Centre de Recherches en Physique des Plasmas, Switzerland
Grauer, Rainer, University of Düsseldorf, Germany
Ivonin, Igor, Uppsala University, Sweden
Klinger, Thomas, Greifswald University, Germany
Kontar, Eduard P., University of Oslo, Norway
Moestam, Robert, Chalmers University of Technology, Sweden
O'Neil, Tom, University of California, USA
Pécseli, Hans, University of Oslo, Norway
Saffman, Mark, University of Wisconsin-Madison, USA
Schröder, Christiane, Greifswald University, Germany
Senchenko, Sergey, University of Uppsala, Sweden

## 2.6 Publications

### 2.6.1 International publications

*Bergeron, K.; Coutsias, E.A.; Lynov, J.P.; Nielsen, A.H.*, Dynamical properties of forced shear layers in an annular geometry. *J. Fluid Mech.* (2000) v. 402 p. 255-289.

*Lynov, J.P.; Bergeron, K.; Coutsias, E.A.; Nielsen, A.H.*, An accurate and efficient spectral method for studies of the dynamical properties of forced, circular shear layers. *Appl. Num. Math.* (2000) v. 33 p. 175-181.

### 2.6.2 Unpublished Danish lectures

*Basse, N.P.; Zoletnik, S.; Saffman, M.; Endler, M.*, Density fluctuations during confinement changes in the Wendelstein 7-AS stellarator. In: Programme. Abstracts. List of participants. Danish Physical Society annual meeting 2000, Nyborg (DK), 8-9 Jun 2000. (HCØ Tryk, København, 2000) AF10.

*Korsholm, S.B.; Cunningham, G.; Michelsen, P.K.; Juul Rasmussen, J.,* Density fluctuation measurements in the mega amp spherical tokamak. In: Programme. Abstracts. List of participants. Danish Physical Society annual meeting 2000, Nyborg (DK), 8-9 Jun 2000. (HCØ Tryk, København, 2000) AF06.

*Michelsen, P.K.,* Fusionsenergi - er det en mulighed. Foredrag for gymnasieklasse fra Tønder Gymnasium, Lyngby (DK), 13 Mar 2000. Unpublished.

*Michelsen, P.K.,* Fusionsenergi - er det en mulighed. Foredrag for gymnasieklasse fra Varde Gymnasium, Lyngby (DK), 11 Oct 2000. Unpublished.

*Michelsen, P.K.,* Kursus i plasmafysik. Forelæsningsrække på Danmarks Tekniske Universitet, Institut for Fysik, Lyngby (DK), Sep - Dec 2000. Unpublished.

*Naulin, V.,* Numerical simulation of plasma turbulence. In: Programme. Abstracts. List of participants. Danish Physical Society annual meeting 2000, Nyborg (DK), 8-9 Jun 2000. (HCØ Tryk, København, 2000) AF08.

### 2.6.3 Unpublished international lectures

*Basse, N.P.; Zoletnik, S.; Saffman, M.; Endler, M.,* Density fluctuations during confinement changes in the Wendelstein 7-AS stellarator. In: Abstracts of invited and contributed papers. 27. European Physical Society conference on controlled fusion and plasma physics, Budapest (HU), 12-16 Jun 2000. Szegö, K.; Todd, T.N.; Zoletnik, S. (eds.), (KFKI-Research Institute for Particle and Nuclear Physics, Budapest, 2000) p. 325.

*Juul Rasmussen, J.,* Turbulent equipartition and anomalous transport in electrostatic turbulence. Meeting at Alfvén Laboratory, Royal Institute of Technology, Stockholm (SE), 28 Feb 2000. Unpublished.

*Juul Rasmussen, J.,* Turbulent equipartition and anomalous transport in electrostatic turbulence. Seminar, Institut für Ionenphysik, Innsbruck (AT), 19 May 2000. Unpublished.

*Juul Rasmussen, J.,* Electrostatic waves and turbulence in plasmas. Course at Institut für Ionenphysik, Innsbruck Universität (14 lectures), Innsbruck (AT), May 2000. Unpublished.

*Juul Rasmussen, J.,* Introduction, turbulence in fluids and plasmas. Workshop on plasma turbulence, anomalous transport, and numerical modeling, Risø (DK), 5-7 Dec 2000. Unpublished.

*Juul Rasmussen, J.; Naulin, V.,* Particle dispersion and density flux in electrostatic drift-wave turbulence. 35. Nordic plasma- and gas discharge symposium, Wadahl (NO), 30 Jan - 2 Feb 2000. Unpublished.

*Juul Rasmussen, J.; Naulin, V.,* Turbulent equipartition and pinch fluxes in pressure driven electrostatic turbulence. International workshop on chaotic transport and complexity, Carry le rouet (FR), 26-30 Jun 2000. Unpublished. Abstract available.

*Korsholm, S.B.,* Introduction to fusion energy and fusion research. Visit from Stenhus Gymnasium at Culham Science Centre, Culham (GB), 27 Mar 2000. Unpublished.

*Korsholm, S.B.,* Introduction to fusion energy and fusion research. Visit from Tørring Amtsgymnasium at Culham Science Centre, Culham (GB), 12 Apr 2000. Unpublished.

*Korsholm, S.B.,* Reflectometry measurements of turbulence in MAST. Workshop on plasma turbulence, anomalous transport, and numerical modeling, Risø (DK), 5-7 Dec 2000. Unpublished.

*Korsholm, S.B.; Michelsen, P.K.; Naulin, V.; Juul Rasmussen, J.,* Reynolds stress and shear flow generation. In: Abstracts of invited and contributed papers. 27. European Physical Society conference on controlled fusion and plasma physics, Budapest (HU), 12-16 Jun 2000. Szegö, K.; Todd, T.N.; Zoletnik, S. (eds.), (KFKI-Research Institute for Particle and Nuclear Physics, Budapest, 2000) p. 375.

*Michelsen, P.K.*, Status of the fusion research. Workshop on plasma turbulence, anomalous transport, and numerical modeling, Risø (DK), 5-7 Dec 2000. Unpublished.

*Naulin, V.*, Transport barrier and flux statistics in a turbulent equipartition model (invited paper). 13. US Transport Task Force workshop, Burlington, VT (US), 26-29 Apr 2000. Unpublished.

*Naulin, V.*, Transport und Dispersion idealer Teilchen in 2-dimensionaler Turbulenz. Meeting at IPP Greifswald, Greifswald (DE), 22 Feb 2000. Unpublished.

*Naulin, V.*, Formation of flows out of turbulence in fluids and plasmas. Workshop on plasma turbulence, anomalous transport, and numerical modeling, Risø (DK), 5-7 Dec 2000. Unpublished.

*Naulin, V.*, Physics of drift-Alfvén turbulence. Workshop on plasma turbulence, anomalous transport, and numerical modeling, Risø (DK), 5-7 Dec 2000. Unpublished.

*Naulin, V.*, Generation of flows from turbulence. Ringberg IPP Theorie Seminar, Tegernsee (DE), 13-17 Nov 2000. Unpublished.

*Naulin, V.*, Generation of flows from turbulence. Meeting at University of St Andrews, Solar and Magnetospheric Theory Group, St Andrews (GB), 22 Nov 2000. Unpublished.

*Naulin, V.; Jessen, T.; Michelsen, P.K.; Nielsen, A.H.; Juul Rasmussen, J.*, Anomalous diffusion of particles and the relation to transport in vortex dominated turbulence. International congress on plasma physics (ICPP-2000) combined with 42. Annual meeting of the Division of Plasma Physics of the American Physical Society, Quebec City (CA), 23-27 Oct 2000. Unpublished.

*Naulin, V.; Juul Rasmussen, J.*, 3D driftwave turbulence simulations at Risø. 35. Nordic plasma- and gas discharge symposium, Wadahl (NO), 30 Jan - 2 Feb 2000. Unpublished.

*Naulin, V.; Juul Rasmussen, J.*, Transport and particle diffusion in vortex dominated driftwave turbulence. International workshop on chaotic transport and complexity, Carry le rouet (FR), 26-30 Jun 2000. Unpublished. Abstract available Naulin, V.; Nycander, J.; Juul Rasmussen, J., Transport barriers and turbulent equipartition. International congress on plasma physics (ICPP-2000) combined with 42. Annual meeting of the Division of Plasma Physics of the American Physical Society, Quebec City (CA), 23-27 Oct 2000. Unpublished.

*Naulin, V.; Scott, B.*, Benchmarking codes for drift Alfvén turbulence. 7. EU-US Transport Task Force workshop: Transport in fusion plasmas - transport barriers physics, Varenna (IT), 4-7 Sep 2000. Unpublished.

*Nielsen, A.H.*, Vortex dynamics and turbulence in two-dimensional flows. Workshop on plasma turbulence, anomalous transport, and numerical modeling, Risø (DK), 5-7 Dec 2000. Unpublished.

*Okkels, F.*, Shell models for turbulence. Workshop on plasma turbulence, anomalous transport, and numerical modeling, Risø (DK), 5-7 Dec 2000. Unpublished.

*Schröder, C.; Klinger, T.; Block, D.; Piel, A.; Bonhomme, G.; Naulin, V.*, Taming drift wave turbulence: Experiment and simulation. International congress on plasma physics (ICPP-2000) combined with 42. Annual meeting of the Division of Plasma Physics of the American Physical Society, Quebec City (CA), 23-27 Oct 2000. Unpublished.

### 2.6.4 Internal reports

*Korsholm, S.B.; Cunningham, G.*, First results of the MAST fluctuation reflectometer. MAST-OPS-Note-00.17 (2000) vp.

# 3. Fusion Technology

## 3.1 Introduction

The work reported in this section has been carried out in the Materials Research Department. The overall objective of the research activities in this area is to determine the impact of neutron irradiation on physical and mechanical properties of metals and alloys, so that appropriate materials can be chosen for their application in an irradiation environment (e.g. in a fusion reactor). Various experimental techniques are employed to study different aspects of the microstructural evolution during irradiation and the resulting consequences on the post-irradiation physical and mechanical properties of metals and alloys. Computer simulations are carried out to understand the evolution of surviving defects and their clusters in collision cascades. The kinetics of defect accumulation during irradiation and the influence of irradiation-induced defects and their clusters on the deformation behaviour of irradiated metals and alloys are studied theoretically. In the following, the main results of these activities are highlighted.

## 3.2 Next Step Technology

### 3.2.1 Impact of creep-fatigue interaction on materials performance and lifetime[1]

*B.N. Singh, J.F. Stubbins* (*University of Illinois, Urbana-Champaign, USA) and P. Toft*

Currently, two copper alloys, one dispersion strengthened Glid Cop CuAl-25 and one precipitation hardened CuCrZr, are being evaluated for their use in the first wall and divertor components of ITER. In service, both these components will be exposed to an intense flux of fusion (14 MeV) neutrons and will experience thermo-mechanical cyclic loading as a result of the cyclic nature of plasma burn operations of the system. Consequently, the structural materials in the reactor vessel will have to endure not only cyclic loading but also stress relaxation and microstructural recovery, (i.e. creep) during the "plasma-on" and "plasma-off" periods. In order to evaluate the impact of this interaction (i.e. creep-fatigue), investigations were initiated to determine the lifetime of CuAl-25 and CuCrZr alloys under the condition of creep-fatigue interaction.

Creep-fatigue interaction studies were performed on 39 mm long fatigue specimens with a gauge length and diameter of 7 and 3 mm, respectively. Fatigue specimens of the CuAl-25 alloy were prepared from the material supplied by OGM Americas (formerly SCM Metals, USA), whereas specimens of the CuCrZr alloy were manufactured from the stock supplied by Outokumpu OY (Finland). The CuCrZr alloy was used in the prime aged condition. Creep-fatigue interaction tests were carried out on unirradiated as well as irradiated specimens. Neutron irradiations were performed in the DR-3 reactor at Risø at 250°C to a dose level of ~0.3 dpa. Irradiated specimens were tested (in vacuum) at 250°C whereas unirradiated specimens were tested at room temperature (22°C) as well as 250°C. CuCrZr specimens were tested only at 250°C and in the unirradiated condition.

[1] Task GB8-V63 (BL12.2) and TWO-T507-5

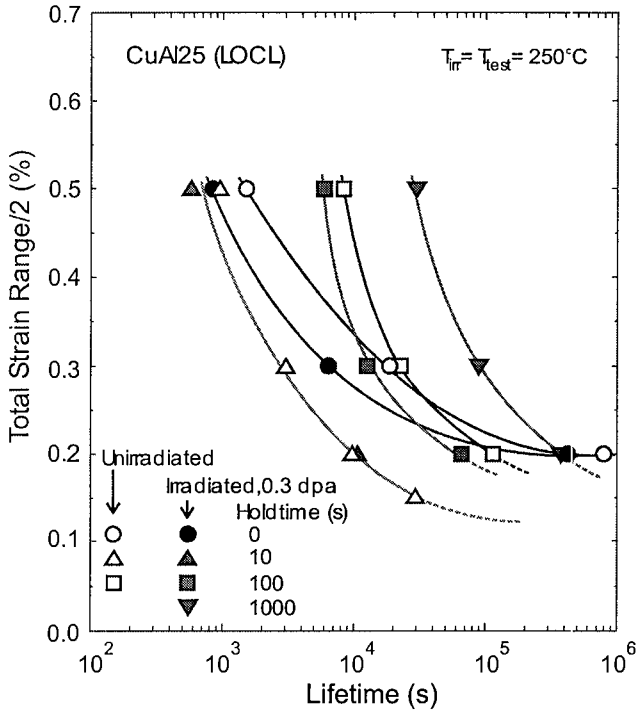


Figure 14. Fracture lifetime as a function of strain range in creep-fatigue interaction tests with different holdtime carried out at 250°C on the dispersion strengthened CuAl-25 alloy.

The creep-fatigue interaction condition was simulated by applying a certain holdtime on both tension and compression sides of the cyclic loading with a frequency of 0.5 Hz for zero hold-time. Tests were carried out in the fully reversed and strain controlled mode. Holdtimes of 10, 100 and 1000 seconds were used. For a given holdtime, the number of cycles to failure was determined at different strain amplitudes. Results of such tests carried out on CuAl-25 at 250°C both in unirradiated and irradiated conditions are shown in Figure 14. In order to demonstrate the impact of holdtime, the real lifetime of the material and the number of creep fatigue cycles to failure are plotted directly as a function of holdtime in Figure 15 for the strain range values of 0.5% (Figure 15a) and 0.2% (Figure 15b).

The results clearly demonstrate that the creep-fatigue interaction has a drastic effect on materials performance and lifetime, particularly at the lower strain range values. As it can be seen in Figure 15, at the strain range value of 0.2% (representing a low loading condition in service), a holdtime of only 10 seconds reduces the number of cycles to failure by three orders of magnitude; even the real lifetime is reduced by almost two orders of magnitude. Even at the higher strain range value of 0.5% (representing a high loading condition in service), the number of cycles to failure decreases by a factor of more than ten for the holdtime of 10s.

Figure 16 shows the results of creep-fatigue interaction tests on the unirradiated CuAl-25 alloy carried out at 22°C at a strain range value of 0.5%. The impact of holdtime on the lifetime as well as the number of cycles to failure is even more drastic than that at 250°C for the strain range value of 0.5%.

Some limited number of creep-fatigue interaction tests have been carried out also on the prime aged CuCrZr alloy at 250°C. Results of tests at 250°C at the strain range of 0.5% are shown in Figure 17. Evidently, the impact of 10s holdtime on the number of cycles to failure is as drastic as in the case of the CuAl-25 alloy.

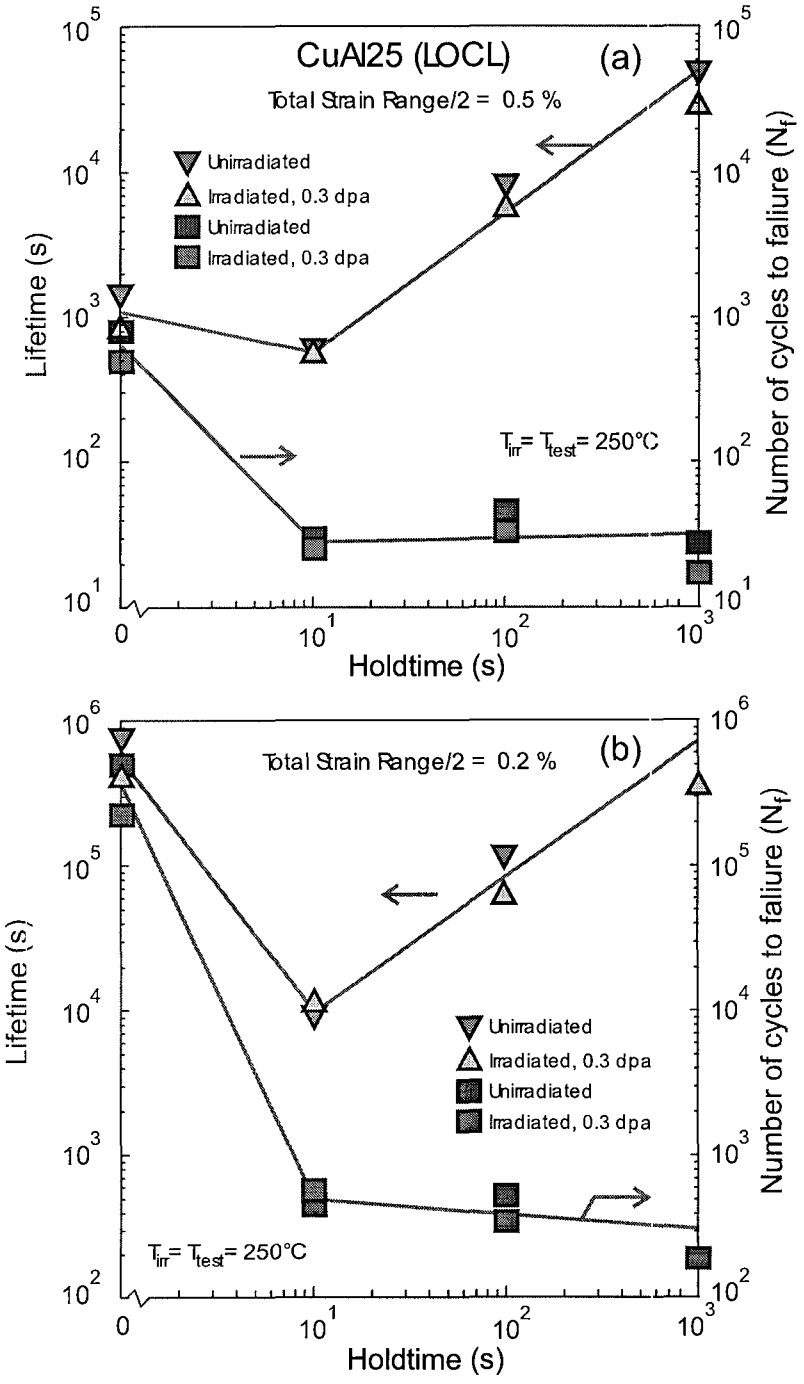


Figure 15. Fracture lifetime and number of cycles to failure as a function of holdtime obtained during creep-fatigue interaction tests at 250°C on CuAl-25 alloy. Results are shown for both unirradiated and irradiated materials tested at two different strain range values.

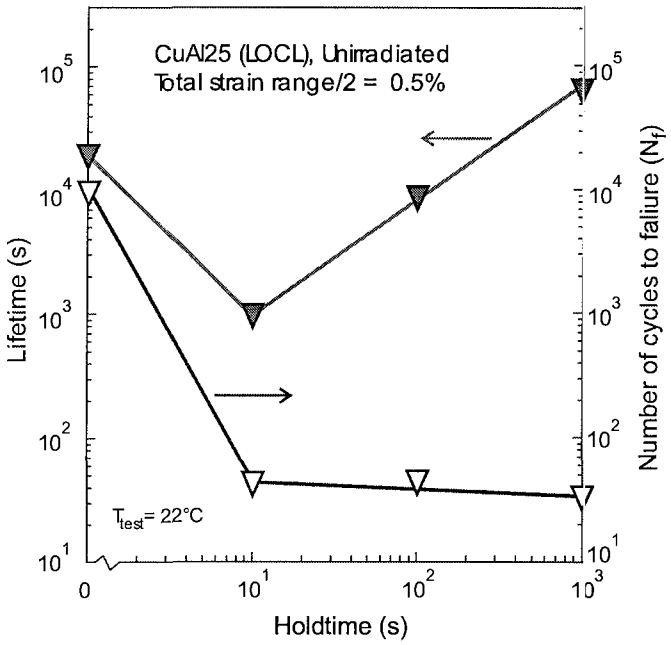


Figure 16. The same as Figure 15, but for tests carried out only on unirradiated specimens and only one strain range value of 0.5% at 22°C.

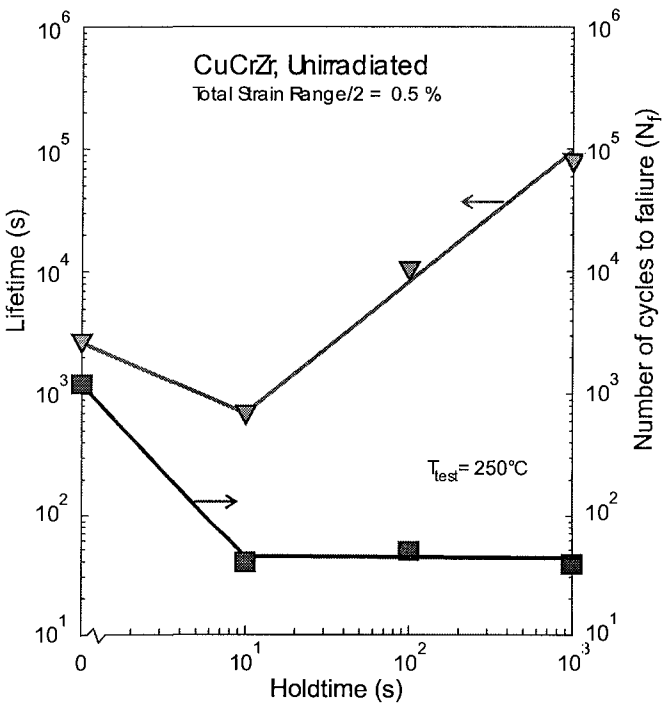


Figure 17. Same as Figure 15, but for tests carried out on prime aged CuCrZr (Outokumpu) alloy in the unirradiated condition at a strain range value of 0.5% at 250°C.

Implications of these results are not very encouraging from the point of view of practical applications of these alloys in structural components of ITER. Furthermore, at present, neither the origin nor the mechanism of this powerful effect of creep-fatigue interaction are known. Further investigations are in progress to help clarify the situation.

### 3.2.2 Low cycle fatigue behaviour of titanium alloys before and after irradiation[2]

*B.N. Singh, J.F. Stubbins* (*University of Illinois, Urbana-Champaign, USA) and P. Toft*

Based on an attractive combination of thermophysical, mechanical and radioactivity decay properties, titanium alloys have been identified as candidate structural materials for different components in fusion reactors. More specifically, two classical and industrially available alloys, namely Ti5Al2.5Sn and TiGAl4V alloys, are being considered as candidate materials for flexible mechanical connectors between the blanket modules and the backplate of ITER. Since not much is known about the effect of neutron irradiation on the phase stability, defect accumulation and mechanical properties of these alloys, screening experiments were initiated to determine the response of these alloys to neutron irradiation at 50 and 350°C. The effect of neutron irradiation on tensile properties of these alloys has been reported earlier and in the following the low cycle fatigue behaviour of these alloys at 50 and 350°C both in the unirradiated and irradiated conditions is described.

Fatigue specimens of α (Ti5Al2.5Sn) and (α+β) (Ti6Al4V) alloys were irradiated with fission neutrons in the DR-3 reactor at Risø at 50 and 350°C to a dose level of 0.3 dpa. Both unirradiated and irradiated specimens were fatigue tested at 50 and 350°C in a vacuum of ~$10^{-5}$ torr with a cyclic loading frequency of 0.5 Hz. Tests were carried out in a strain-controlled mode until fracture occurred. The fracture lifetime (number of cycles to failure) was determined as a function of the applied strain amplitude. The loading cycles were always fully reversed. Fracture surfaces were examined in a scanning electron microscope (SEM) and the deformed bulk microstructure was studied using a transmission electron microscope (TEM).

The fatigue lives of the α-alloy determined at 50 and 350°C in the unirradiated and irradiated conditions are presented in Figure 18. The unirradiated α-alloy exhibits (at a given strain range value) longer lifetime at 350°C than at 50°C, particularly at lower strain range values (compare Figure 18a and Figure 18b). It should be noted that the neutron irradiation to ~0.3 dpa does not seem to affect the fatigue life of the α-alloy at 50°C. In contrast, irradiation at 350°C does shorten the fatigue life, particularly at the higher strain range values.

Figure 19 shows the fatigue performance of the (α+β) alloy tested also at 50 and 350°C in the unirradiated and irradiated conditions. In the case of the unirradiated (α+β) alloy, at higher strain range values, the fatigue life is found to be longer at 50°C than that at 350°C. However, the behaviour reverses at the lower strain range values such that the fatigue life at 350°C (at a given strain range value) is longer than that at 50°C. In the case of (α+β) alloy, irradiation at 50°C to ~0.3 dpa causes a significant increase in the fatigue life at lower strain range values. At 350°C, on the other hand, irradiation does not seem to have any effect on the fatigue life of the (α+β) alloy tested at any strain range value. This is rather surprising in view of the fact that the irradiation at 350°C to ~0.3 dpa causes a very significant increase in the tensile strength of the (α+β) alloy.

It should be noted that whereas the unirradiated α and (α+β) alloys behave very similarly at 50°C, their fatigue performance at 350°C differs significantly. The unirradiated α-alloy, for example, has noticeably longer fatigue lives than the (α+β) at 350°C at the higher strain range values.

[2] Task V61 (BL14.2)

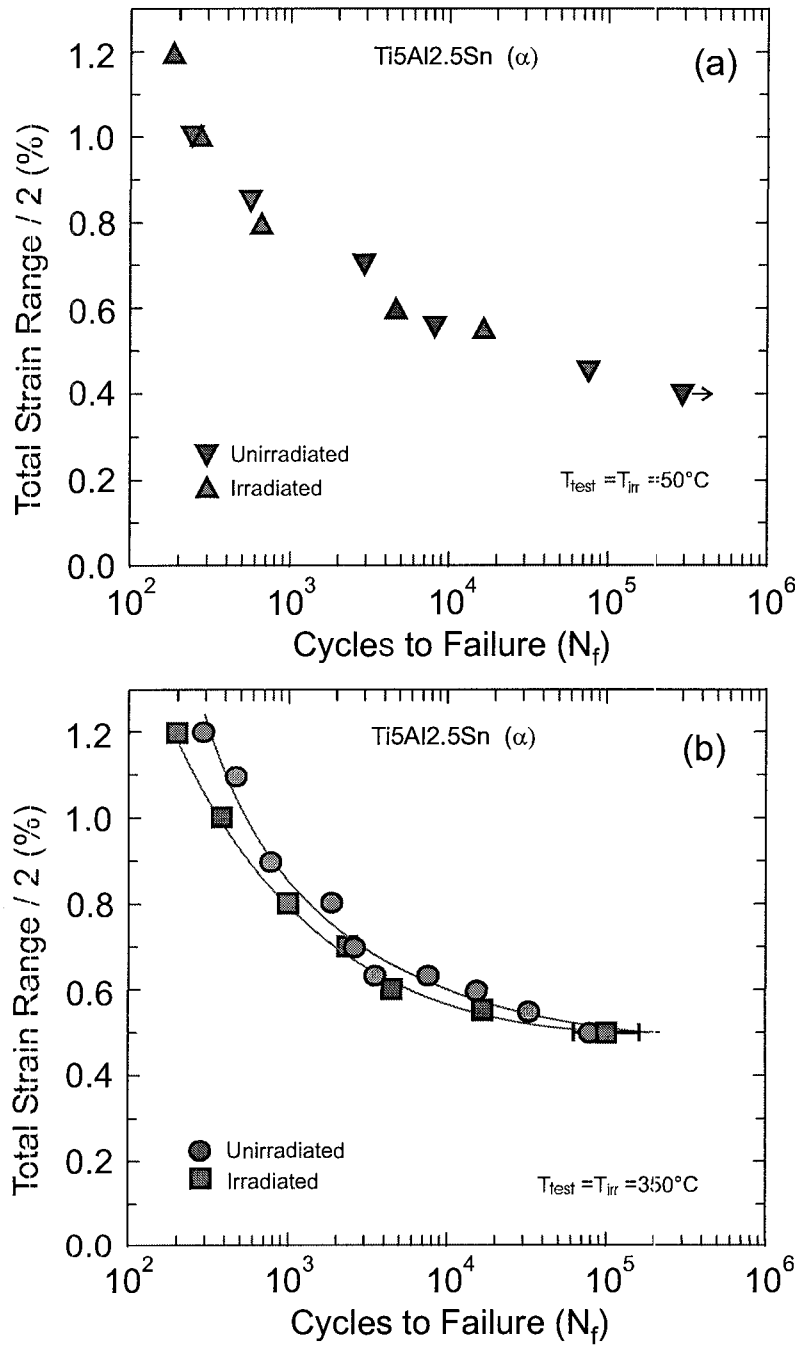


Figure 18. Fatigue lives of the α(Ti5Al2.5 Sn) titanium alloy determined at 50 and 350°C in the unirradiated and irradiated conditions.

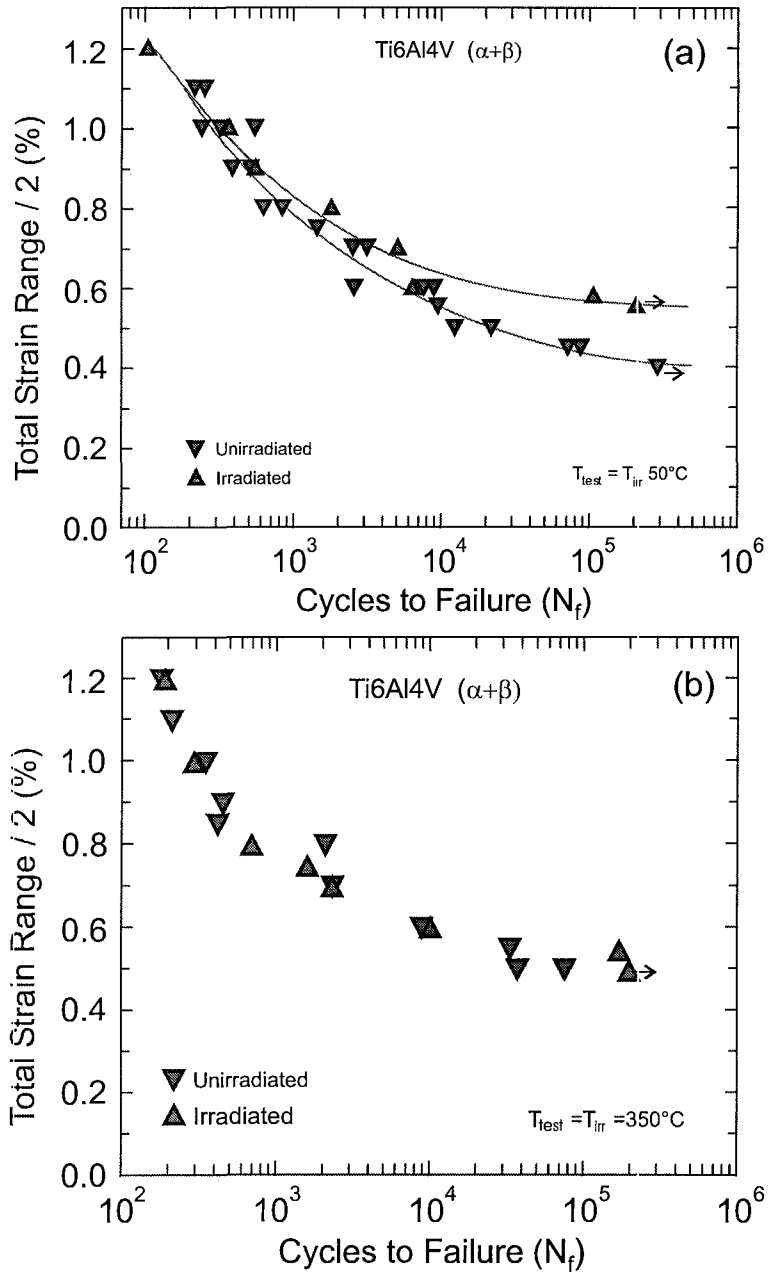


Figure 19. Same as Figure 18 but for the (α+β) (Ti6Al4V) titanium alloy.

### 3.2.3 Fracture toughness behaviour of unirradiated and irradiated titanium alloys[3]

*S. Tähtinen*, P. Moilanen* (*VTT Manufacturing Technology, Finland) and B.N. Singh*

In addition to the work reported in section 3.2.2, the fracture toughness behaviour of these two titanium alloys was also investigated at 50 and 350°C both before and after neutron irradiation. Fracture toughness specimens (3 x 4 x 27 mm) were irradiated in the DR-3 reactor at Risø to a dose level of ~0.3 dpa at 50 and 350°C. Fracture resistance curves were determined using the displacement controlled three-point bend tests with a constant

[3] Task V61 (BL14.2)

displacement rate of 2.5 x $10^{-4}$ mm $s^{-1}$. Fracture resistance testing at elevated temperatures were carried out in a silicon oil bath. Load, displacement and crack length measured using the DC-PD method were recorded during the testing and the fracture resistance curves were determined following the ASTM Standard Test Method for J-Integral Characterization of Fracture Toughness, E1737-96.

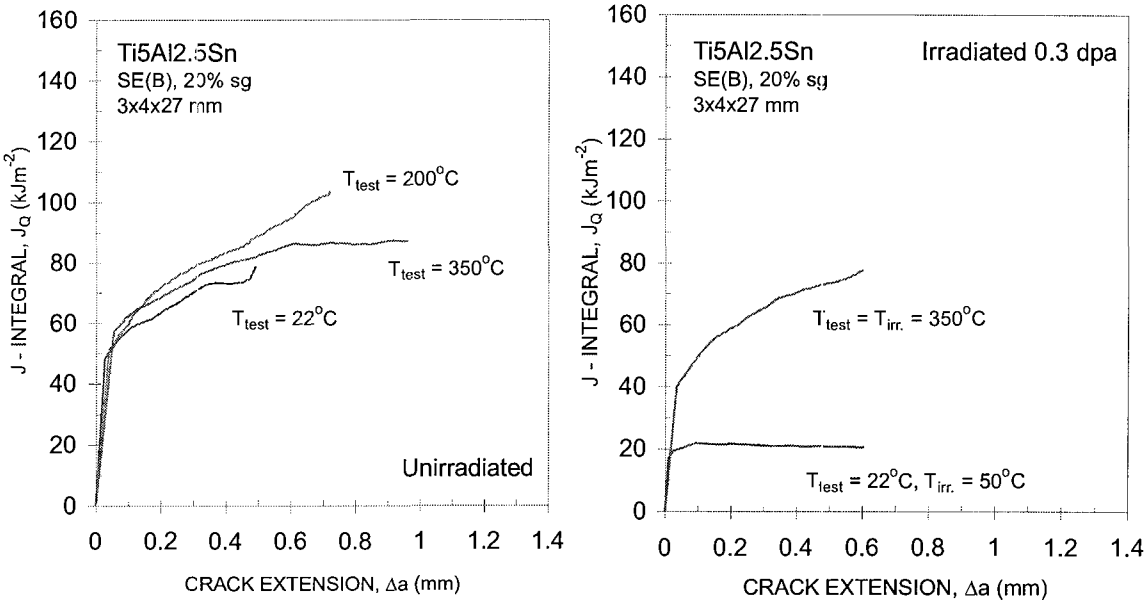


Figure 20. Fracture resistance curves for α-titanium alloy at different test temperatures in the unirradiated and neutron irradiated conditions.

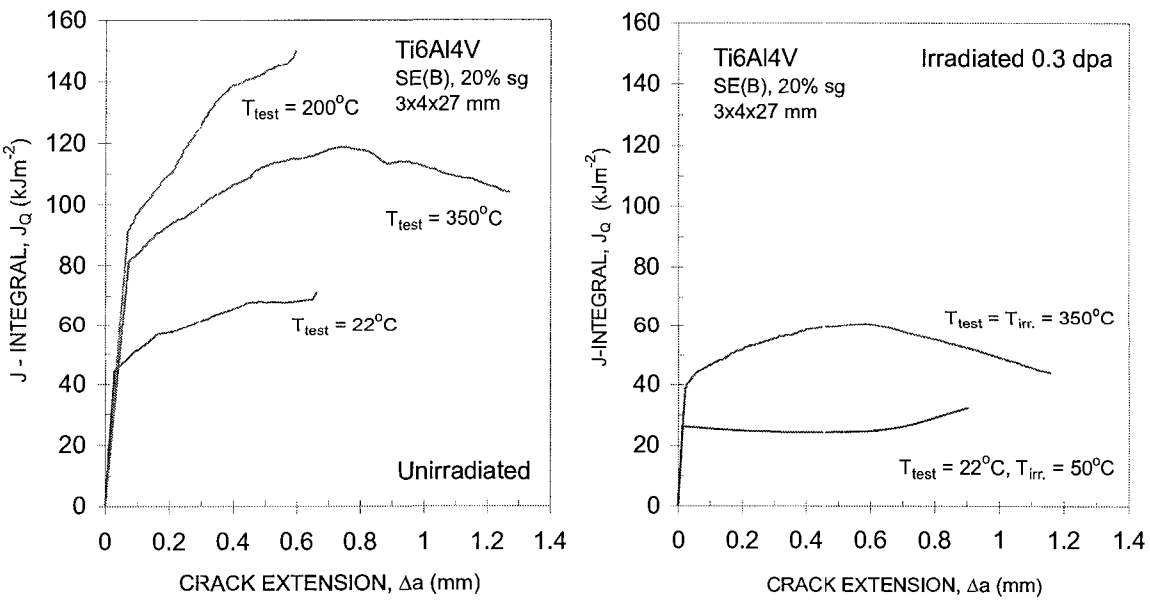


Figure 21. The same as Figure 20 but (α+β)-titanium alloy.

The effect of temperature and neutron irradiation on the fracture resistance behaviour of α (Ti5Al2.5Sn) and (α+β) (Ti6Al4V) alloys are shown in Figure 20 and Figure 21, respectively. In the unirradiated condition the α- and (α+β) alloys have similar fracture toughness properties at 22°C (see Figure 20a and Figure 21a). However, at 250°C, the fracture toughness of the α-alloy is slightly lower than that of the (α+β) alloy. Neutron irradiation at 50°C to a dose level of ~0.3 dpa causes hardening and reduction in fracture toughness in both α- and (α+β) alloys. Irradiation at 350°C resulted in substantial hardening and significant decrease in the fracture toughness of the (α+β) alloy, whereas only minor changes in fracture toughness behaviour was observed in the α-alloy. The fracture toughness properties of (α+β) alloy seem to be more strongly affected by neutron irradiation than that of the α-alloy. The preliminary results indicate that this may have its origin in the irradiation induced precipitation in the (α+β) alloy at the irradiation temperature of 350°C. The present results suggest that the phase stability in the (α+β) alloy during irradiation should be further investigated.

## 3.3 Long Term Technology

### 3.3.1 Decoration of dislocations with defect clusters in bcc iron[4]

*N.M. Ghoniem* (*University of California, Los Angeles, USA) and B.N. Singh*

It is well established that neutron irradiation of metals and alloys leads to a substantial increase in the yield strength and a significant decrease in the ductility when irradiated at temperatures below the recovery stage V (i.e. about 0.3 $T_m$ for iron where $T_m$ is the melting temperature in Kelvin). It is the decrease in the ductility which is a matter of serious concern from the point of view of application of materials in a fusion reactor environment. Recently, the cascade induced source hardening (CISH) model was proposed to rationalize this phenomenon. This model is based on the premise that during irradiation under cascade damage conditions the grown-in dislocations get decorated with small SIA clusters and that this atmosphere of clusters/loops prevents the grown-in dislocations from acting as dislocation sources. Later it was shown analytically that at least energetically, the grown-in dislocations are likely to get decorated by 1-D diffusing SIA clusters produced in the cascades. However, in the previous work quantitative determination of the mechanisms by which the phenomenon occurs was not investigated in detail.

In the present work, a new computational method known as 3-D Dislocation Dynamics is used to examine the mechanism of interaction between small defect clusters and the grown-in dislocations. This methodology enables calculations of displacements, strains, stresses, interaction and self-energies and the work associated with rotation and translation of defect clusters. Within this framework the temperature dependence of the trapping zone size for small defect clusters has been calculated for bcc iron and molybdenum and the results are presented in Figure 22. As temperature increases, the elastic modulus decreases and the thermal energy of the cluster increases. Both factors co-operate to reduce the effective trapping zone at higher temperatures.

[4] Task TTMS-001

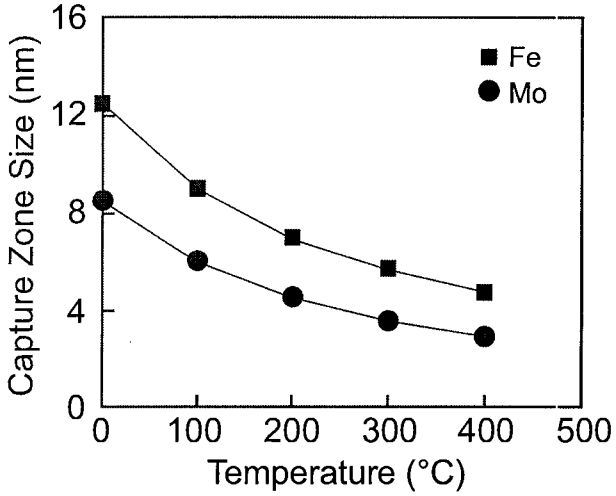


Figure 22. Temperature dependence of the trapping zone size for small defect clusters in bcc iron and molybdenum.

Calculations have shown that in bcc iron clusters will tend to accumulate just below and above the slip plane, depending on their Burgers vector orientation, and on the character of the adjacent dislocation segment. Maximum cluster trapping is shown to occur near the edge component of a grown-in dislocation, while the trapping zone size decreases to zero near purely screw components. Furthermore, it is found that as clusters accumulate near the grown-in dislocation, those clusters that are very close to the dislocation core (within ~3 nm) are likely to be absorbed into the core. Simulations show that this would happen because of the rotation of the Burgers vector of these loops as a result of unbalanced torque exerted on them by the grown-in dislocation. The accuracy of the present results needs to be examined by atomistic simulations since our assumption of linear isotropic elasticity may not be exactly valid when considering loop-dislocation interaction so close to the dislocation core.

### 3.3.2 Dislocation-loop interaction in bcc iron[5]

*Yu. N. Osetsky*, D.J. Bacon* (*The University of Liverpool, Liverpool, England),*
*A. Serra** (**Universitat Politècnica de Catalunya, Barcelona, Spain) and B.N. Singh*

As indicated in the preceeding section, the interactions between dislocations and defect clusters are important and need to be understood properly in order to predict the mechanical performance of materials under cascade damage conditions. However, it is still not certain as to whether or not these interactions can be treated accurately within the framework of isotropic linear elasticity theory. To help eliminate this uncertainty, we have carried out comparative studies of such interactions using atomistic (Molecular Dynamics) simulations and two theoretical approaches based on the simple infinitesimal loop approximation and full isotropic elasticity.

In bcc iron we have studied the interaction of a dislocation with Burgers vector $\underline{b}$ = ½ <111> lying along <112> direction with a SIA cluster with the same Burgers vector $\underline{b}$ situated at different distances below the extra half-plane. First, molecular statics were used to determine the interaction energy at a temperature of zero Kelvin in bcc iron lattice. The crystallites of about a million atoms were oriented along $[1\bar{1}0]$, $[1\,1\bar{2}]$ and [111] directions. The size along the Burgers vector, $\underline{b}$, was about 100/$\underline{b}$/ and approximately 15 nm along the

[5] Task TTMS-001

dislocation line. The usual boundary conditions for static dislocation studies were applied, i.e. periodic along the dislocation line direction and rigid along the other two directions. An isolated dislocation was first introduced and relaxed. A cluster with the same Burgers vector as that of the dislocation was then created at a certain distance, $r_{<110>}$ (e.g. along $[1\bar{1}0]$ [direction) below the dislocation slip plane and the crystallite was relaxed again. A cluster of 37 SIAs (effective loop radius of 1.3 nm) was used, The dislocation – cluster interaction energy was obtained using the energies of a previously-relaxed isolated dislocation and a cluster.

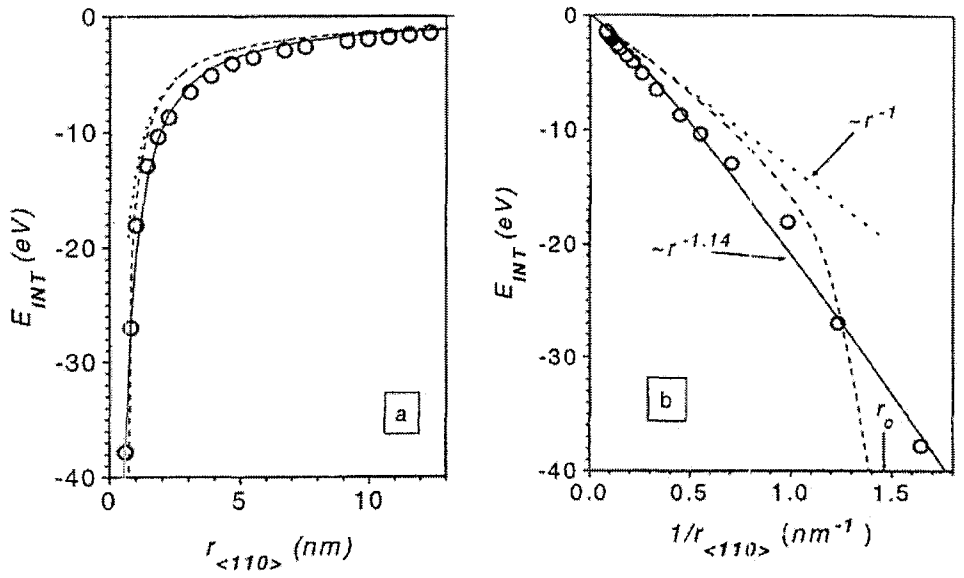


Figure 23. Interaction energy between 1/2 <111> edge dislocation and a perfect loop of 37 SIA in bcc iron as a function of (a) separation distance along <110> direction and (b) reciprocal of the separation distance. Full line (——) power function fitted to the MD simulation data, dashed line (- - - -) full isotropic elasticity calculation and dotted line (.....) infinitesimal loop approximation (reciprocal distance law) calculation.

Figure 23 shows the interaction energy of a 37 SIA cluster with an edge dislocation in bcc iron as a function of the distance $r_{<110>}$ of the cluster from the dislocation. The estimation of the corresponding interaction energy using the infinitesimal loop approximation and the full isotropic elasticity theory is also shown in Figure 23. In Figure 23a all dependencies seem to be in a satisfactory agreement. However, in Figure 23b where the interaction energy is shown versus the reciprocal separation distance, a significant difference, particularly at short distances, can be clearly seen. It is concluded that in the case of bcc iron, full isotropic elasticity calculations give satisfactory results on dislocation-loop interaction energy at distances larger than several dislocation core radii but overestimate the interaction force at short distances. The use of infinitesimal loop approximation, on the other hand, yields satisfactory agreement but only at large distances.

### 3.3.3 Void formation in neutron and proton irradiated pure iron[6]

*M. Eldrup and B.N. Singh*

The problem of void formation in bcc metals and alloys has been the subject of investigations in a number of laboratories. With the aim of obtaining a better understanding of these problems, such as the influence of irradiation temperature, annealing treatment and the presence of gas, a series of experiments on pure iron (and on steel) have been initiated.

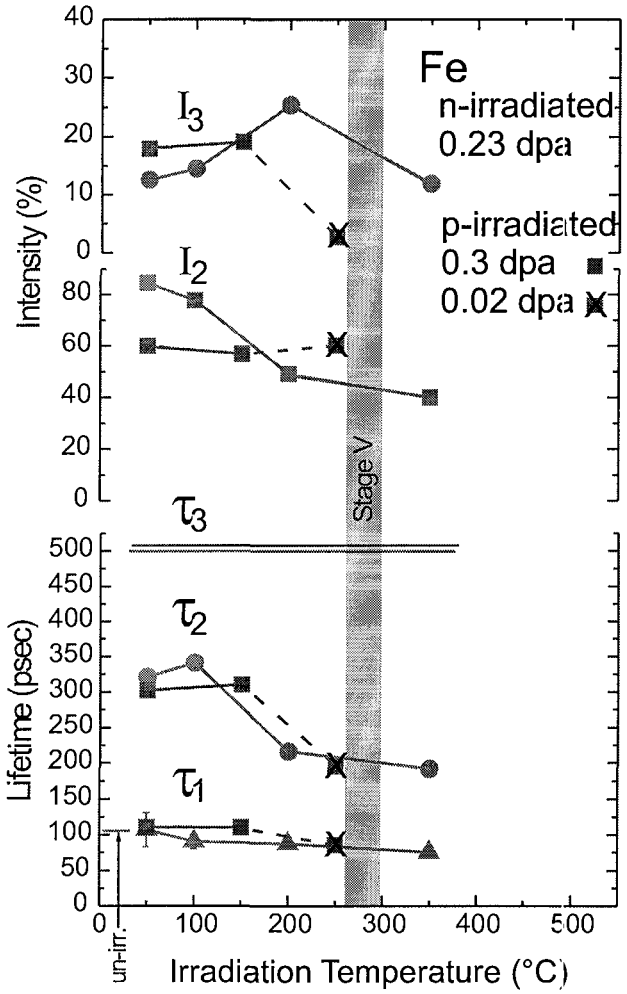


Figure 24. The variation of positron lifetimes and their intensities with irradiation temperature for iron irradiated with neutrons (red) and 600 MeV protons (blue). The lifetimes $\tau_2$ and $\tau_3$ are characteristic for different types of defects. At low temperatures both voids ($\tau_3$ = 500 ps as shown by straight lines) and micro-voids ($\tau_2$ ~300 – 350 ps) are formed, while at higher temperatures no micro-voids are seen. The intensities $I_2$ and $I_3$ of the lifetime components give information about the defect densities.

To study the microstructure of pure iron after neutron and 600 MeV proton irradiation, positron annihilation spectroscopy (PAS) has been applied (in collaboration with CRPP-FTM, Villigen - PSI, Switzerland). PAS has the advantage that it is sensitive to vacancy-type defects such as single vacancies, two-dimensional vacancy clusters (i.e. loops) and three-dimensional vacancy agglomerates (i.e. voids and gas bubbles). With PAS it is possible to detect sub-microscopic voids (microvoids) and get information about their sizes, since the

[6] Task TTMS-001

lifetime of positrons that are trapped in such microvoids increases with the cavity size in the range from mono-vacancies up to agglomerates of about 50 vacancies. In addition, the technique provides information about the density of such cavities.

The results (see Figure 24) show that in general both neutron and 600 MeV proton irradiations of iron (to doses of 0.23 and 0.3 displacements per atom, respectively) lead to the formation of both microvoids and voids at an irradiation temperature as low as ~ 50°C and up to about 200°C. At temperatures above ~ 200°C, no microvoids are formed and the void density decreases with increasing temperature.

The microvoids typically have average sizes of ~ 10 - 15 vacancies, while the voids on average contain more than ~ 50 vacancies. The density of the voids is 3 - 8 times smaller than that of the microvoids, both being in excess of $10^{23}$ $m^{-3}$ for irradiation temperatures below ~ 200°C. If the total microvoid and void population is considered, the average cavity size is larger in the proton than in the neutron irradiated iron.. An important conclusion is that although the details of the microstructures differ for the two types of irradiation, the created void populations are qualitatively the same.

# 3.4 Underlying Technology

### 3.4.1 Effects of one-dimensional glide on the reaction kinetics of interstitial clusters

*H.L. Heinisch* (*Pacific Northwest National Laboratory, Richland, USA), H. Trinkaus** (**Forschungszentrum Jülich, Jülich, Germany) and B.N. Singh*

Neutron irradiation-induced collision cascades in metals produce small interstitial clusters and perfect dislocation loops that glide in thermally activated, one-dimensional (1D) random walks. These 1D gliding defects can occasionally change their direction of migration by thermal activation or by interactions with other defects. Their migration is therefore "mixed 1D/3D migration" along an overall 3D path consisting of 1D segments. The defect reaction kinetics under mixed 1D/3D migration are different from the reaction kinetics under pure 1D diffusion and pure 3D diffusion, both of which can be formulated within analytical rate theory models of microstructure evolution under irradiation. The existence of mixed 1D/3D migration introduces a new variable into the reaction kinetics: the average distance traveled between direction changes, L. So, in the new analytical theory, the concept of "sink strength" is determined not only by the concentration and properties of the sinks, but also by the kinetic properties of the migrating defects.

Atomic-scale kinetic Monte Carlo (KMC) computer simulations of defect migration are being used to investigate the effects of mixed 1D/3D migration on defect reaction kinetics as a guide for implementing mixed 1D/3D migration into the analytical theory. KMC simulations of idealized systems have been performed to study the functional dependence of sink strengths on the variables affecting the defect-sink interactions under mixed 1D/3D migration. In these KMC studies defects migrate one at a time through the crystal by random hopping to adjacent fcc lattice sites until they are absorbed in randomly distributed unsaturable spherical absorbers of radius R and number density N. The "sink strength" in the simulations is defined in terms of the measured defect lifetime (the average number of hops to absorption) determined in the KMC simulations.

In analytical rate theories for 3D and 1D migration the sink strengths can be expressed in terms of the size and density characteristics of the sink population. The KMC results demonstrate that the dependence of sink strength on the size and concentration of sinks under

mixed 1D/3D migration lies between those for pure 1D and pure 3D migration and varies with L.

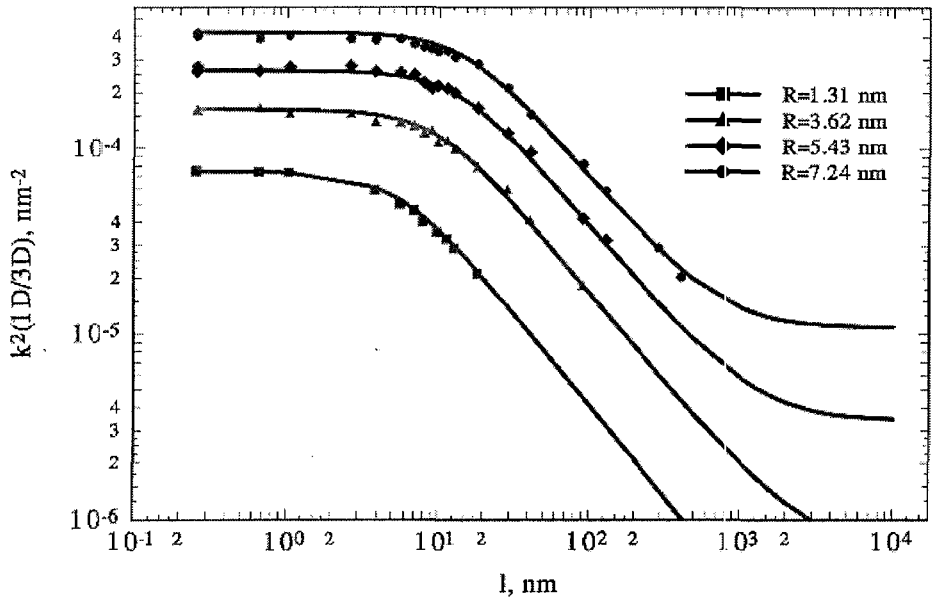


Figure 25. A comparison of the analytical expression (curves) and computer simulation results (points) for the sink strength of a random array of absorbers of number density, N, and radius, R, as a function of L, the ID path length of migrating defects under mixed 1D 3D migration. Data for four different values of R are shown.

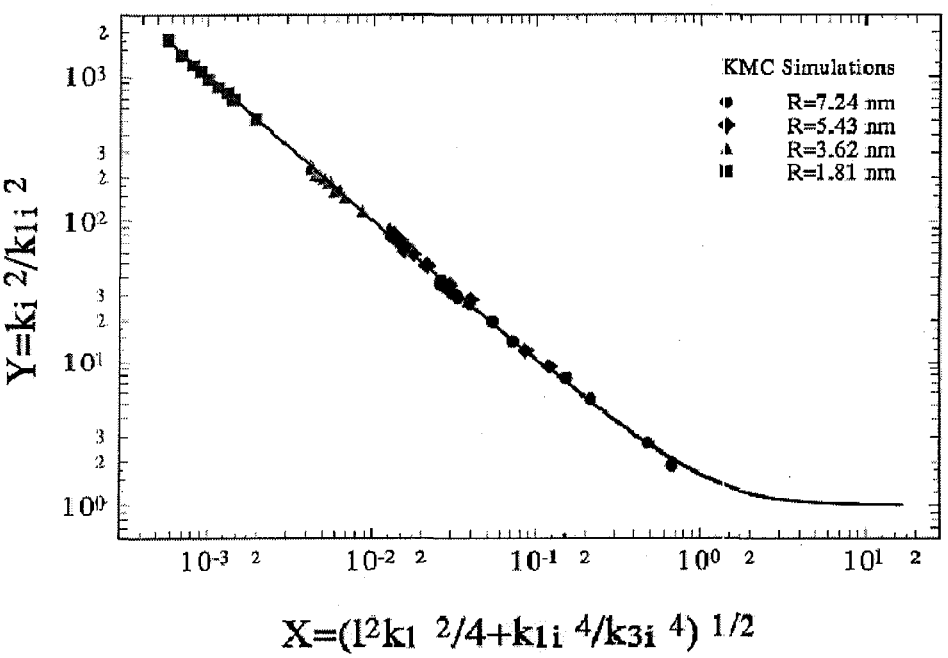


Figure 26. The Master Curve relating 3D and 1D reaction kinetics. Data points are the results of KMC simulations shown in Figure 25 and the full line is the result of analytical calculations.

A new analytical theory has been developed, based on physical arguments independent of the computer simulations, that describes the sink strength from pure 3D, through mixed 1D/3D, to pure 1D as a function of L, and it can be expressed in terms of the sink strengths for pure 1D and pure 3D. Figure 25 is a plot of the sink strengths determined in KMC simulations as a function of L for several values of R. The new analytical expression for the sink strength under mixed 1D/3D migration fits the KMC results perfectly. A master curve has been developed onto which the simulation data for all values of R collapse, Figure 26.

### 3.4.2 Radiation hardening and plastic flow localization in fcc metals and alloys

*N.M. Ghoniem*, S.-H. Tong* (*University of California, Los Angeles, USA), B.N. Singh and L.Z. Sun** (**The University of Iowa, Iowa City, USA)*

Experimentally it is well established that neutron irradiation of metals and alloys at temperatures below the recovery stage V causes a large increase in the upper yield stress (radiation hardening), and beyond a certain dose level, induces a yield drop. The initiation of plastic deformation in these irradiated materials occurs in a very localized fashion and in the form of cleared channels. This kind of the localized plastic flow causes a drastic decrease in ductility of irradiated materials. In order to rationalize these observations, the cascade induced source hardening (CISH) model was proposed.[7] The present work was initiated to validate the CISH model and extend it to understand the plastic flow localization using 3-D Dislocation Dynamics. Using this methodology, we have investigated the dynamics of dislocation interaction with radiation-induced defect clusters, and specifically with (a) SIA clusters in dislocation decoration and (b) stacking fault tetrahedra ($SFT_s$ randomly distributed in the matrix.

The present investigations have shown that dislocation lines are highly flexible. For small inter-cluster or stand-off distances (which are typical of decorated dislocations), the unlocking stress can be a factor of two smaller than values obtained when one assumes rigid dislocation interactions in the analytical calculations. Two possible mechanisms of dislocation un-locking have been identified: (1) an asymmetric unzipping-type instability caused by partial decoration of dislocations; (2) a fluctuation-induced morphological instability, when the dislocation line is extensively decorated by defect clusters. Estimated unlocking stress values are in general agreement with experimental observations that show a yield drop behaviour. It appears that unlocking of heavily decorated dislocations will be most prevalent in areas of stress concentration (e.g. precipitate, grain boundary, triple point junction, or surface irregularity).

Computer simulations for the interaction between unlocked F-R sources and a 3-D random field of SFTs have been utilized to estimate the magnitude of radiation hardening, and to demonstrate a possible mechanism for the initiation of localized plastic flow channels. Reasonable agreement with experimental hardening data has been obtained with the critical angle $\phi_c$ in the limited range of $158^\circ - 165^\circ$ (see Figure 27). Both the magnitude and dose dependence of the increase in flow stress by neutron irradiation at 50°C and 100°C are reasonably well predicted. In spatial regions of internal high stress, or on glide planes of statistically-low SFT densities, unlocked dislocation sources can expand and interact with SFTs. Dislocations drag atomic-size jogs and/or small glissile SIAs when an external stress is applied. High externally-applied stress can trigger point-defect recombination within SFT volumes resulting in local high-temperatures. A fraction of the vacancies contained in SFTs can therefore be absorbed into the core of a gliding dislocation segment producing atomic-

[7] B.N. Singh, A.J.E. Foreman and H. Trinkaus, J. Nucl. Mater. 251 (1997) 103.

size jogs and segment climb. The climb height is a natural length scale dictated by the near-constant size of the SFT in irradiated copper. It is shown by the present computer simulations that the width of a dislocation channel is on the order of 200 – 500 atomic planes, as observed experimentally, and is a result of a stress-triggered climb/glide mechanism. The atomic details of the proposed dislocation-SFT interaction and ensuing absorption of vacancies into dislocations need further investigations by atomistic simulations.

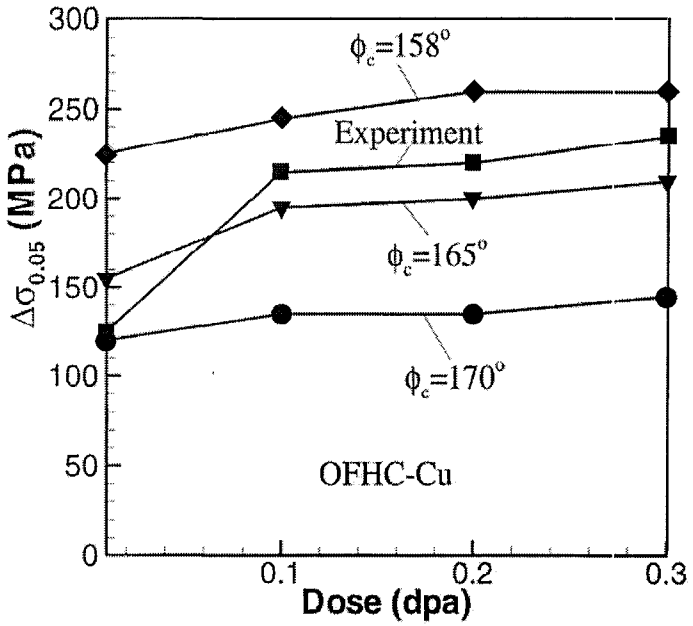


Figure 27. Comparison between the dose dependence of the calculated increase in flow stress (due to irradiation) values and the experimental measurements of Singh, Edwards and Toft (unpublished work).

Finally, it should be pointed out that at relatively high neutron doses, dense decorations of dislocations with SIA loops, and a high density of defect clusters/loops in the matrix are most likely to occur. As shown here, these conditions can lead to the phenomena of yield drop and flow localization. Solutions of these problems in the field of materials design may be sought, either to avoid dislocation decorations and channel formation, or to prevent propagation of dislocations through the channels (e.g. by providing closely-spaced indestructible obstacles on glide planes).

### 3.4.3 Effect of grain size on void swelling under cascade damage conditions

*B.N. Singh, M. Eldrup, S.J. Zinkle* (*Oak Ridge National Laboratory, Oak Ridge, USA) and S.I. Golubov** (**IPPE, Obninsk, Russia)*

The effect of grain size on void swelling has its origin in the intrinsic property of grain boundaries as neutral and unsaturable sinks for both vacancies and self-interstitial atoms (SIAs). The phenomenon was investigated already in the 1970s[8] and it was demonstrated that the grain size dependent void swelling measured under irradiation producing only Frenkel pairs could be satisfactorily explained in terms of the standard rate theory (SRT) and

[8] B.N. Singh, Nature, Physical Science, 224 (1973) 142; Phil.Mag. 29 (1974) 25.

dislocation bias[9]. Experimental results reported in the 1980s demonstrated, on the other hand, that the effect of grain size on void swelling under cascade damage conditions was radically different[10] and could not be explained in terms of the SRT.

In an effort to understand the source of this intriguing and significant difference, the effect of grain size on void swelling under cascade damage conditions has been investigated both experimentally and theoretically in pure copper irradiated with fission neutrons at 350°C to a dose level of ~0.3 dpa. The post-irradiation defect microstructure including voids was investigated using transmission electron microscope (TEM) and positron annihilation spectroscopy (PAS). The evolution of void swelling was calculated both analytically and numerically within the framework of the production bias model (PBM) and the SRT. The theoretical treatment has been formulated such that both the local void swelling in the grain interiors (determined directly from TEM measurements) and the volumetric average swelling for the whole grain (determined from PAS or density change measurements) can be calculated. Results of the numerical calculations of void swelling for both the local and the average void swelling as a function of grain size are presented in Figure 28 and Figure 29.

It can be clearly seen from Figure 28 and Figure 29 that both the local and the average void swelling calculated using the PBM agree quite well with the experimentally measured grain size dependence of void swelling. This agreement can be considered as a direct evidence in support of the PBM.

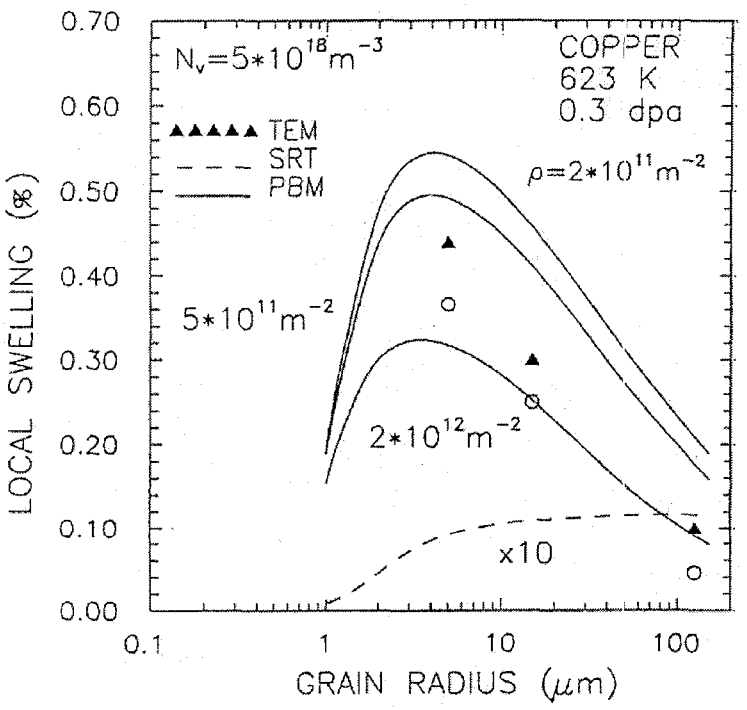


Figure 28. The calculated (full lines) and experimentally measured (▲) grain size dependence of the local void swelling in the grain interiors of copper irradiated at 350°C to 0.3 dpa. The open circles (O) are the swelling values calculated for specific grain sizes using the experimental values of void and dislocation densities.

[9] B.N. Singh and A.J.E. Foreman, Phil.Mag. 29 (1974) 847.
[10] A. Horsewell and B.N. Singh, ASTM-STP 955 (1987) 220.

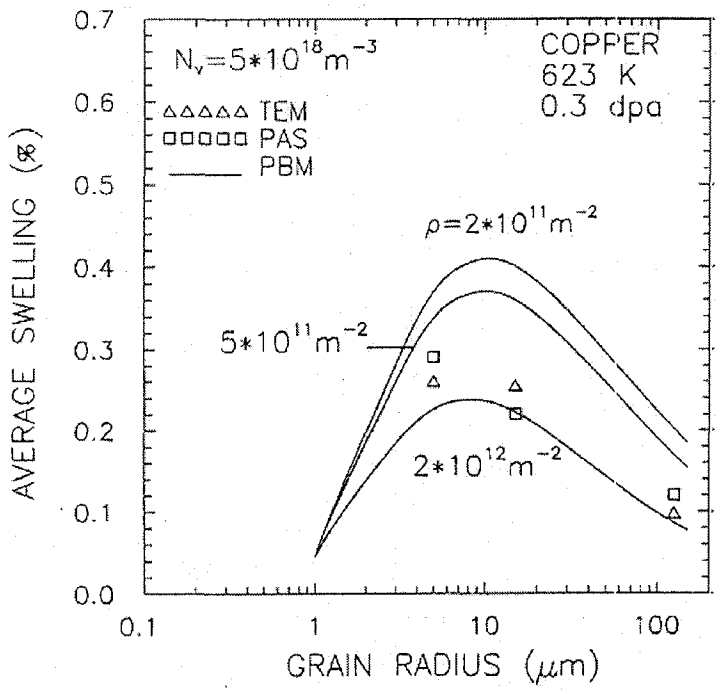


Figure 29. The grain size dependence of the average void swelling calculated (full lines) using PBM and measured experimentally using TEM (Δ) and PAS ( □).

The present work has led to two significant conclusions: (a) that the nature of the grain size effect on void swelling is directly related to the features of the primary damage production and the properties of the resulting defect clusters in displacement cascades and (b) that under cascade damage conditions, the grain size effect on void swelling is an intrinsic effect and covers a wide range of grain sizes extending upto 100 μm or even larger. The second conclusion implies that while selecting materials for structural components in a fission or fusion reactor, the problem of grain size effect should be carefully evaluated.

## 3.5 Participants in Fusion Technology

### 3.5.1 Scientific staff

| | |
|---|---|
| Eldrup, M. | (part time ~70%) |
| Singh, B.N. | |
| Toft, P. | (part time ~70%) |

### 3.5.2 Technical staff

| | |
|---|---|
| Lindbo, J. | (part time ~20%) |
| Nilsson, H. | (part time ~10%) |
| Olsen, B, F. | |
| Pedersen, N.J. | (part time ~40%) |

### 3.5.3 Guest scientists

Edwards, D.J., Pacific Northwest National Laboratory, Richland, USA
Heinisch, H.L., Pacific Northwest National Laboratory, Richland, USA
Ishino, S., Tokai University, Kanagawa-ken, Tokyo, Japan
Stubbins, J.F., University of Illinois, Urbana-Champaign, USA

## 3.6 Publications and Conference Contributions

### 3.6.1 International publications


Almazouzi, A.; Rubia, T.D. de la; Singh, B.N.; Victoria, M., Basic aspects of differences in irradiation effects between fcc, bcc and hcp metals and alloys. Editors' summary. International workshop on basic aspects of differences in irradiation effects between FCC, BCC and HCP metals and alloys, Asturias (ES), 15-20 Oct 1998. J. Nucl. Mater. (2000) v. 276 p. 295-296.

Edwards, D.J.; Singh, B.N., Overaging of Outokumpu CuCrZr. In: Fusion materials. Semiannual progress report for the period ending June 30, 2000. DOE/ER-0313/28 (2000) p. 176-182.

Edwards, D.J.; Singh, B.N.; Toft, P., Radiation hardening in HCP titanium alloys. In: Fusion materials. Semiannual progress report for the period ending June 30, 2000. DOE/ER-0313/28 (2000) p. 214-220.

Eldrup, M.; Singh, B.N., Study of defect annealing behaviour in neutron irradiated Cu and Fe using positron annihilation and electrical conductivity. International workshop on basic aspects of differences in irradiation effects between FCC, BCC and HCP metals and alloys, Asturias (ES), 15-20 Oct 1998. J. Nucl. Mater. (2000) v. 276 p. 269-277.

Ghoniem, N.M.; Singh, B.N.; Sun, L.Z.; Rubia, T.D. de la, Interaction and accumulation of glissile defect clusters near dislocations. International workshop on basic aspects of differences in irradiation effects between FCC, BCC and HCP metals and alloys, Asturias (ES), 15-20 Oct 2000. J. Nucl. Mater. (2000) v. 276 p. 166-177.

Ghoniem, N.M.; Singh, B.N.; Sun, L.Z.; Rubia, T. D. de la, Dislocation decoration with nano-scale defect clusters in irradiated metals. In: Fusion materials. Semiannual progress report for the period ending December 31, 1999. DOE/ER-0313/27 (2000) p. 222-223.

Ghoniem, N.M.; Sun, L.Z.; Singh, B.N.; Tong, S.-H., Investigations of radiation hardening and plastic instability in FCC metals. In: Fusion materials. Semiannual progress report for the period ending December 31, 1999. DOE/ER-0313/27 (2000) p. 226-228.

Golubov, S.I.; Singh, B.N.; Trinkaus, H., Defect accumulation in fee and bcc metals and alloys under cascade damage conditions. Towards a generalisation of the production bias model. International workshop on basic aspects of differences in irradiation effects between FCC, BCC and HCP metals and alloys, Asturias (ES), 15-20 Oct 1998. J. Nucl. Mater. (2000) v. 276 p. 78-89.

Heinisch, H.L.; Singh, B.N.; Golubov, S.I., Kinetic Monte Carlo studies of the effects of Burgers vector changes on the reaction kinetics of one-dimensionally gliding interstitial clusters. International workshop on basic aspects of differences in irradiation effects between FCC, BCC and HCP metals and alloys, Asturias (ES), 15-20 Oct 1998. J. Nucl. Mater. (2000) v. 276 p. 59-64.

Heinisch, H.L.; Singh, B.N.; Golubov, S.I., The effects of one-dimensional glide on the reaction kinetics of interstitial clusters. J. Nucl. Mater. (2000) v. 283-287 p. 737-740.

Heinisch, H.L.; Singh, B.N.; Golubov, S.I., The effects of one-dimensional glide on the reaction kinetics of interstitial clusters. In: Fusion materials. Semiannual progress report for the period ending December 31, 1999. DOE/ER-0313/27 (2000) p. 211-213.

Osetsky, Y.N.; Bacon, D.J.; Serra, A.; Singh, B.N.; Golubov, S.I., Stability and mobility of defect clusters and dislocation loops in metals. International workshop on basic aspects of differences in irradiation effects between FCC, BCC and HCP metals and alloys, Asturias (ES), 15-20 Oct 1998. J. Nucl. Mater. (2000) v. 276 p. 65-77.

Osetsky, Y.N.; Bacon, D.J.; Gao, F.; Serra, A.; Singh, B.N., Study of loop-loop and loop-edge dislocation interactions in bcc iron. J. Nucl. Mater. (2000) v. 283-287 p. 784-788.

Osetsky, Y.N.; Serra, A.; Singh, B.N.; Golubov, S.I., Structure and properties of clusters of self-interstitial atoms in fcc copper and bcc iron. Phil. Mag. A (2000) v. 80 p. 2131-2157.

Singh, B.N.; Eldrup, M.; Horsewell, K.; Ehrhart, P.; Dworschak, F., On recoil energy dependent void swelling in pure copper. Part 1. Experimental results. Phil. Mag. A (2000) v. 80 p. 2629-2650.

Sun, L.Z.; Ghoniem, N.M.; Tong, S.-H.; Singh, B.N., 3D dislocation dynamics study of plastic instability in irradiated copper. J. Nucl. Mater. (2000) v. 283-287 p. 741-745.

Trinkaus, H.; Singh, B.N.; Golubov, S.I., Progress in modelling the microstructural evolution in metals under cascade damage conditions. J. Nucl. Mater. (2000) v. 283-287 p. 89-98.

Tähtinen, S.; Laukkanen, A.; Singh, B.N., Damage mechanisms and fracture toughness of GlidCop CuAl25 IG0 copper alloy. J. Nucl. Mater. (2000) v. 283-287 p. 1028-1032.

Tähtinen, S.; Singh, B.N.; Toft, P., Effect of neutron irradiation on mechanical properties of Cu/SS joints after single and multiple HIP cycles. J. Nucl. Mater. (2000) v. 283-287 p. 1238-1242.

Victoria, M.; Baluc, N.; Bailat, C.; Dai, Y.; Luppo, M.I.; Schaublin, R.; Singh, B.N., The microstructure and associated tensile properties of irradiated fcc and bcc metals. International workshop on basic aspects of differences in irradiation effects between FCC, BCC and HCP metals and alloys, Asturias (ES), 15-20 Oct 1998. J. Nucl. Mater. (2000) v. 276 p. 114-122.

Zinkle, S.J.; Singh, B.N., Microstructure of Cu-Ni alloys neutron irradiated at 210°C and 420°C to 14 dpa. J. Nucl. Mater. (2000) v. 283-287 p. 306-312.

### 3.6.2 Danish reports

Golubov, S.I.; Singh, B.N.; Trinkaus, H., On recoil energy dependent void swelling in pure copper: Theoretical treatment. Risø-R-1186(EN) (2000) 30 p.

Singh, B.N.; Edwards, D.J.; Eldrup, M.; Toft, P., Comparison of properties and microstructures of Tréfimétaux CuNiBe and Hycon 3HP™ before and after neutron irradiation. Risø-R-1049(EN) (2000) (ITER R&D Task No. T213) 31 p.

Singh, B.N.; Stubbins, J.F.; Toft, P., Low cycle fatigue behaviour of neutron irradiated copper alloys at 250 and 350° C. Risø-R-1128(EN) (2000) (ITER R&D Task No. T213) 54 p.

### 3.6.3 Foreign books and reports

Almazouzi, A.; Victoria, M.; Rubia, T.D. de la; Singh, B.N. (eds.), Proceedings. International workshop on basic aspects of differences in irradiation effects between FCC, BCC and HCP metals and alloys, Asturias (ES), 15-20 Oct 1998. (Elsevier, Amsterdam, 2000) (Journal of Nuclear Materials, v. 276) 306 p.

Tähtinen, S.; Singh, B.N., Tensile and fracture toughness properties of copper alloys to stainless steel joints. BVAL62-001030 (2000) 14 p.

Tähtinen, S.; Singh, B.N., Effects of multiple hip thermal cycles and neutron irradiation on mechanical properties of copper alloys joint to stainless steel. BVAL62-001062 (2000) 12 p.

### 3.6.4 Conference proceedings

Schiøtz, J.; Leffers, T.; Singh, B.N., Modeling of dislocation generation and interaction during high-speed deformation of metals. In: Proceedings. 3. Workshop on high-speed plastic deformation, Hiroshima (JP), 7-9 Aug 2000. (Hiroshima Institute of Technology, Hiroshima, 2000) p. 307-316.

Singh, B.N., Impacts of cascade producing irradiations on microstructural modifications and global performance of materials. In: Proceedings. Vol. 2. International symposium on materials ageing and life management (ISOMALM 2000), Kalpakkam (IN), 3-6 Oct 2000. Raj, B.; Rao, K.B.S.; Jayakumar, T.; Dayal, R.K. (eds.), (Allied Publishers Ltd., Mumbai, 2000) p. 823-836.

Singh, B.N.; Stubbins, J.F.; Toft, P., Fatigue behavior of copper alloys with and without exposure to neutrons. In: Proceedings. Vol. 2. International symposium on materials ageing and life management (ISOMALM 2000), Kalpakkam (IN), 3-6 Oct 2000. Raj, B.; Rao, K.B.S.; Jayakumar, T.; Dayal, R.K. (eds.), (Allied Publishers Ltd., Mumbai, 2000) p. 862-868.

Tähtinen, S.; Singh, B.N., Tensile and fracture behaviour of high strength copper alloys and their joints with 316 L(N) stainless steel. In: Proceedings. Vol. 3. International symposium on materials ageing and life management (ISOMALM 2000), Kalpakkam (IN), 3-6 Oct 2000. Raj, B.; Rao, K.B.S.; Jayakumar, T.; Dayal, R.K. (eds.), (Allied Publishers Ltd., Mumbai, 2000) p. 1080-1086.

### 3.6.5 Unpublished lectures

Eldrup, M.; Singh, B.N., Void nucleation in fcc and bcc metals: A comparison of neutron irradiated copper and iron. 12. International conference on positron annihilation, München (DE), 6-11 Aug 2000. Unpublished. Abstract available.

Eldrup, M.; Singh, B.N., Damage accumulation in pure iron and F82H steel under neutron irradiation. IEA international workshop on reduced activation ferritic/martensitic steels for fusion structural applications, Tokyo (JP), 2-3 Nov 2000. Unpublished.

Ghoniem, N.M.; Tong, S.-H.; Trinkaus, H.; Singh, B.N., A computational method for 3-D parametric dislocation dynamics and its application to flow localization. Dislocation 2000 - International conference on the fundamentals of plastic deformation, National Institute of Standards and Technology, Gaithersburg, MD (US), 19-22 Jun 2000. Unpublished. Abstract available.

Ghoniem, N.M.; Tong, S.; Singh, B.N.; Trinkaus, H., Computational methods for mesoscopic plastic deformation with applications to flow localization of irradiated materials. IUMRS-2000: International conference in Asia - Multiscale materials modelling symposium, Hong Kong (HK), 24-26 Jul 2000. Unpublished. Abstract available.

Ghoniem, N.M.; Tongo, S.-H.; Singh, B.N.; Huang, J., Mechanisms of radiation-induced hardening and flow localization in irradiated fcc metals. International conference on computational engineering sciences (ICES 2K). Symposium on mechanics of materials from nano to meso scale, Los Angeles, CA (US), 22-25 Aug 2000. Unpublished.

Osetsky, Y.N.; Bacon, D.J.; Singh, B.N., Interactions between edge dislocations and interstitial clusters in bcc-Fe and fcc-Cu. Materials Research Society Fall meeting. Symposium on multiscale materials modeling, Boston, MA (US), 27 Nov - 1 Dec 2000. Unpublished. Abstract available.

Singh, B.N., Report on effect of irradiation on physical and mechanical properties of metals and alloys. Technology monitoring workshop, Garching (DE), 18-19 Jul 2000. Unpublished.

Singh, B.N., Activities, achievements and perspectives in the field of fusion materials technology programme at Risø. Fusion Evaluation Board Meeting, Espo (FI), 18 Feb 2000. Unpublished.

Singh, B.N., Radiation damage and response of materials exposed to energetic projectiles. Meeting at Culham Science Centre, UKAEA Fusion, Culham (GB), 23 Mar 2000. Unpublished. Abstract available.

Singh, B.N., Flow localization and plastic instability in irradiated metals and alloys. International workshop on dislocation - defect interaction in irradiated materials, Toledo (ES), 3-5 Apr 2000. Unpublished.

Singh, B.N., Microstructural evaluation in fcc and bcc metals and alloys under cascade damage conditions. International workshop on production and accumulation of defects under cascade damage conditions, Barcelona (ES), 7-9 Sep 2000. Unpublished.

Trinkaus, H.; Heinisch, H.L.; Singh, B.N., Analytical and Monte Carlo studies of the effects of direction changes on the defect reaction kinetics of 1-D migrating defect. Materials Research Society Fall meeting. Symposium on multiscale materials modeling, Boston, MA (US), 27 Nov - 1 Dec 2000. Unpublished. Abstract available.

Tähtinen, S.; Laukkanen, A.; Singh, B.N., Qualification of copper to stainless steel joints. 21. Symposium on fusion technology, Madrid (ES), 11-15 Sep 2000. Unpublished. Abstract available.

**Bibliographic Data Sheet** **Risø-R-1283(EN)**

Title and authors

Association Euratom – Risø National Laboratory
Annual Progress Report 2000

Edited by J.P. Lynov and B.N. Singh

| ISBN | ISSN |
|---|---|
| 87-550-2917-5<br>87-550-2918-3 (Internet) | 0106-2840 |

| Department or group | Date |
|---|---|
| Optics and Fluid Dynamics Department | August 2001 |

| Pages | Tables | Illustrations | References |
|---|---|---|---|
| 45 | | 29 | 19 |

Abstract (max. 2000 characters)

The programme of the Research Unit of the Fusion Association Euratom - Risø National Laboratory covers work in fusion plasma physics and in fusion technology. The fusion plasma physics group has activities within development of laser diagnostics for fusion plasmas and studies of nonlinear dynamical processes related to turbulence and turbulent transport in the edge region of magnetised fusion plasmas. The activities in technology cover investigations of radiation damage of fusion reactor materials. These activities contribute to the Next Step, the Long-term and the Underlying Fusion Technology programme. A summary is presented of the results obtained in the Research Unit during 2000.

Descriptors INIS/EDB

LASER DOPPLER ANEMOMETERS; MAGNETIC CONFINEMENT; NONLINEAR PROBLEMS; NUMERICAL SOLUTION; PELLET INJECTION; PHYSICAL RADIATION EFFECTS; PLASMA DIAGNOSTICS; PLASMA SCRAPE-OFF LAYER; PLASMA SIMULATION; PROGRESS REPORT; RISOE NATIONAL LABORATORY; THERMONUCLEAR REACTOR MATERIALS; TOKAMAK DEVICES; TURBULENCE; VORTICES

Available on request from Information Service Department, Risø National Laboratory,
(Afdelingen for Informationsservice, Forskningscenter Risø), P.O.Box 49, DK-4000 Roskilde, Denmark.
Telephone +45 4677 4004, Telefax +45 4677 4013, email: risoe@risoe.dk